Solitons in non-linear media and their coherent control

A Thesis Submitted to

NIRMA UNIVERSITY

for the degree of

Doctor of Philosophy in PHYSICS

BY

Utpal Roy

Under the Supervision of

Dr. Prasanta K. Panigrahi

THEORETICAL PHYSICS DIVISION
PHYSICAL RESEARCH LABORATORY,
AHMEDABAD - 380 009, INDIA

DECEMBER, 2007

(Refer R.Ph D 3.5 of Academic Regulations for Ph D study)

CERTIFICATE

1. This is to certify that I, UTPAL ROY, am registered as a student under Registration No; 05EXTPHDS07 for Doctoral programme under the institute of SCIENCE under the Nirma University of Science & Technology. I have completed the research work and also the pre-synopsis seminar as prescribed under the regulation no: 3.5 for the Ph. D study.

2. It is further certified that the work embodied in this thesis is original and contains the independent investigations carried out by me. The research is leading to the * discovery of ~~new~~ facts/ techniques / correlation of scientific facts already known.

   * (Please tick whichever is applicable)

Date: 19.12.2007

Utpal Roy
Signature of the student

Forwarded By Guide:

Prasanta K. Panigrahi
DR. PRASANTA K. PANIGRAHI (Guide)

Remarks of Head of the Department (if any):

Date: 19/12/2007 **Signature:**

Remarks of Dean Faculty of Doctoral Studies & Research (if any):

Date: 19/12 **Signature:**

To,
The Executive Registrar
Nirma University

While submitting the above certificate the research scholar & Guide are required to refer regulation no: R.Phd 3.6 if the research work is covered under that Regulation, then a separate certificate incorporating the details about the work which has been already submitted elsewhere for a degree in his various thesis covering wide field, is required.

to
my parents

Contents

Acknowledgement vi

Abstract viii

1 Introduction 1

1.1 Solitons 1

1.2 Bose-Einstein condensates 3

1.3 Gross-Pitaevskii equation 6

2 Coherent control of solitons in strongly coupled cigar-shaped BEC 12

2.1 Introduction 12

2.2 Exact solitons of the strongly coupled BEC 14

2.2.1 Connection between Lieb-mode of weakly coupled BEC and soliton in the Thomas-Fermi sector 17

2.3 Coherent control of the solitons 19

2.4 Stability of the dark soliton 22

3 Complex solitons in Bose-Einstein condensates with two- and three-body interactions 28

3.1 Introduction 28

3.2 Power-law complex soliton 30

3.3 Algebraic soliton in a lossy trap 34

3.4 Stability of solitons: 35

4 Vibrations as probe of Bose-Einstein condensates in different phases 40

4.1 Introduction 40

4.2 Faraday waves in weakly coupled BEC 41

4.3 Faraday waves in BEC with strong and three-body interactions 42

5 Sinusoidal Excitations in Two Component Bose-Einstein Condensates 45

5.1 Introduction 45

5.2 Sinusoidal Solutions of coupled GP equations 47
5.3 Solutions in presence of Harmonic oscillator trap 48
5.4 Solutions in presence of an Optical lattice 51

6 Coherent states of Pöschl-Teller potential and their revival dynamics 57
6.1 Introduction 57
6.2 Algebraic structure of quantum mechanical potential problems 59
6.3 Coherent state for the symmetric-Pöschl-Teller potential 62
6.4 Revival dynamics of coherent state 64

7 Sinusoidal excitations in reduced Maxwell-Duffing model 74
7.1 Introduction 74
7.2 Reduced Maxwell-Duffing Model: 76
7.3 Fractional Linear Transform and the solutions: 77

Conclusions and Future Outlook 83

List of Publications 87

Acknowledgement

First of all, I would like to express my sincere gratitude to my thesis supervisor Dr. Prasanta K. Panigrahi. I will be grateful forever for his tremendous help, guidance and teaching. It was a great opportunity to learn from his deep insight in the subject, excitements in new findings and working out everything from the first principle. His ability for guiding students is exceptional. His encouragement for regular academic discussion among the students and exchanging our results have created a nice academic environment. I respect his punctuality everywhere in his daily life. I have gained a lot from his beautiful teaching, starting from the course-work in my first year of PRL. Sometimes, I get surprise by his tremendous analytical ability and connecting it to various interdisciplinary physical applications. I am greatly benefited from the discussions with him and his encouraging and inspiring words, for which I will always be indebted to him.

I would like to thank Dr. J. Banerji for his constant encouragement and valuable support. I am deeply grateful for his advise, inspiration and constant help. I always respect his meticulous nature. His friendly nature and cheerful company make my stay pleasant at PRL. Throughout my work, his comments and suggestions have been of valuable help to me. I also thank Mrs. Banerji (Swati di) for being cordial and cooperative all the times.

I thank Dr. R. P. Singh (R. P. ji) for being caring and extremely helpful all the times. He is always friendly and encouraging. I also thank Prof. G. S Agarwal and Dr. Bimalendu Deb (Bimalendu da) for their help and constant encouragement. I sincerely thank the academic committee members and all faculty members in PRL. I am also grateful to Prof. A. K. Singhvi, Prof. S. Rindani and Dr. P. Sharma for their kind help and support.

It is of great pleasure to thank all stuff members of library, computer center

and administration for their excellent co-operation and constant help; to name a few: Mr. Y. M Trivedi, Mr. Rangnathan, late Purobi di, Mrs. Uma Desai, Sudheen ji, Babubhai, Ghanshyam bhai, Keyurbhai and so many.

I owe my heartfelt thanks to my seniors Shubhrangshu da and Asoka di. They have been very caring and I am privileged to have their affection. I cherish every moment spent with them. Their company had made my stay in PRL a joy forever.

I also humbly acknowledge Kaushik da for a good and memorable time. It was always a pleasant experience to discuss with him irrespective of academic and non-academics. I am thankful for his care, concerns and company and will always cherish the wonderful moments we had together.

I thank all my affectionate juniors, specially Ayan, Bhaswar, Priyam, Suman, Suratna, Subimal, Amzad, Sumanta, Waliur, Sanat, Sasadhar, Rabiul and few others. I would also like to extend my thanks to all my friends and colleges Charan, Rajneesh, Tarak da, Soloman, Manimaran, Subhendu, Jaiswal, Arun, Vivek, Sudheesh, Pathak, Tarun, Sanjoy, Jitendra, Ashok, and Manan.

Finally, I am deeply indebted to my parents for their continuous support and encouragement. The love and care they showered on me is beyond words. I am grateful to my elder brothers and sisters who have been a constant source of moral support, encouragement and inspiration. I also remember with pleasure the real love and affection of my nephews and nieces (Tanku, Riku, Kano, and Mimi) for providing me joyful moments.

Last but not the least, my appreciation to my wife, Suranjana, for her unconditional love, profound understanding and constant inspiration. No words, perhaps can express my appreciation for her love, affection and endless help. She always takes my problem as her own, help me to overcome them, and encourage me to achieve a high level. This work would not have been completed without her help and support.

Utpal Roy

Abstract

Solitons and solitary waves manifest in dynamical systems, when dispersion and non-linearity balance each other. These solutions of non-linear equations, which arise in diverse physical systems, can be localized or continuous. Bose-Einstein condensate (BEC) is one of the very well studied non-linear systems, where atom-atom interactions lead to rich structures. The formation dynamics and control of these waves in BEC are subjects of intense current research. The order parameter equation governing the dynamics of mean field BEC is the Gross-Pitaevskii equation, a non-linear generalization of the familiar Schrödinger equation. Other than BEC, non-linear Schrödinger equation (NLSE) manifests in non-linear fibre optics [1, 2]. Wave propagation in resonant and non-resonant atomic media is another area governed by non-linear equations.

Developing analytical tools for finding the solutions of aforementioned systems and analyzing their properties have been the goal of this thesis. In this context, we first study the strongly coupled cigar shaped Bose-Einstein condensate. Finding exact soliton solutions and a procedure for their coherent control have been achieved. Control and manipulation of BEC have been achieved through the distributed non-linearity, gain/loss and other parameters of the system. Power law-type complex soliton is then found for a quasi-one-dimensional Bose-Einstein condensate with both two and three-body interactions. We then study this system in a harmonic trap and find that the solution retains its self- similar character. Subsequently, we explore various longitudinal excitations in BEC, resulting from the time dependence of the trap frequency. Two-component BEC is then analyzed, where we have identified new sinusoidal solutions. Their behavior in a trap and periodic lattice are investigated. In particular, we find dynamical super-fluid to insulator phase transition here. Apart from studying the coherent localized solutions of non-linear equations, we have also analyzed the time evolution of a lo-

calized quantum wave packet due to a Hamiltonian whose eigen values are quadratic in the quantum number n. Specifically, we have studied the evolution of the coherent state of the Pösch-Teller potential. The phase-space study reveals sub-Planck structure arising due to fractional revival phenomenon of wave packet. We then focus our attention on another nonlinear system in non-resonant atomic media, the Maxwell-Duffing model. It is found that our procedure enables one to identify a wide class of solutions. These include, sinusoidal and cnoidal wave solutions.

(i) Exact solitons for strongly coupled cigar shaped Bose-Einstein condensates:

In weakly coupled cigar shaped BEC, localized soliton, as well as soliton trains are exact solutions, which have found experimental confirmation, although the formation mechanism of bright solitons, still remains unclear. Unlike the weakly coupled scenario, lack of exact solutions for the strongly coupled case has led to numerical investigations and variational approaches to the Thomas-Fermi limit of the Gross-Pitaevskii (GP) equation [3]. Here, we present exact soliton and soliton train solutions of the strongly coupled cigar shaped BEC. The presence of a harmonic trap, as well as the temporal variation of scattering length, loss/gain and oscillator confinement are treated analytically. This opens up the possibility of coherent control of atom laser in the strongly coupled regime.

(ii) Power-law soliton for cigar shaped BEC both with two- and three-body interactions:

The three-body interaction can be generally treated as a perturbation over the two-body case; it becomes significant for short range and larger scattering length. A number of theoretical studies have been carried out considering three body interaction in both three- and quasi-one-dimensions. We demonstrate the existence of power-law type complex solitons in the presence of repulsive two- and attractive three-body interactions. The dark solitons have a constant velocity determined by the interaction strengths, which is quite different from the Lieb mode case [4]. Their profiles can change as a function of the parameters of the theory.

(iii) Faraday waves in cigar shaped Bose-Einstein conden-

sates:

Temporal variation of scattering length or transverse frequency can lead to Faraday excitations in a cigar shaped BEC [3]. We first study these excitation in strongly coupled BEC and BEC with both two- and three-body interactions. The effect of sudden change in the oscillator frequency is then analytically modelled.

(iv) Sinusoidal Excitations in Two Component Bose-Einstein Condensates

The non-linear coupled Gross-Pitaevskii equation governing the dynamics of the two component Bose-Einstein condensate (TBEC) is shown to admit pure sinusoidal, propagating wave solutions in quasi one dimensional geometry. These solutions, which exist for a wide parameter range, are then investigated in the presence of a harmonic oscillator trap with time dependent scattering length. This illustrates the procedure for coherent control of these modes through temporal modulation of the parameters, like scattering length and oscillator frequency. We subsequently analyzed this system in an optical lattice, where the occurrence of an irreversible phase transition from superfluid to insulator phase is seen.

(v) Coherent states (CSs) of symmetric Pöschl-Teller potential (SPT) and their time evolution:

We make use of novel exponential forms of the solutions of differential equations [5], for identifying the symmetry generators underlying the hypergeometric equation. This is used to construct and study the displacement operator coherent state (DOCS) of the Pöschl-Teller potential [6]. The primary motivation for considering the Pöschl-Teller potential is that, it has a quadratic energy spectrum leading to a rich revival structure for its CS, which can lead to the formation of cat-like states. The temporal evolution, auto-correlation and quantum carpet structures of the CSs are carefully analyzed for delineating their structure and various time scales present in this problem.

(vii) Sinusoidal excitation in a non-resonant atomic medium:

One of the well studied approaches to dense non-resonant atomic medium is to consider the response of the medium as weakly nonlinear. Such situation

leads to the Duffing oscillator model, where the nonlinear response of the medium is assumed to be cubic. On the other hand, the unidirectional wave propagation approximation reduces the Maxwell wave equation from second order to a first order equation. These two, together can well-describe the wave propagation in a non-resonant atomic medium and are called the reduced Maxwell-Duffing model (RMD). We present here mono frequency, sinusoidal wave excitations for RMD system. This excitation exists only in the presence of a polarizing background. General cnoidal wave solutions are found both with and without background.

Chapter 1

Introduction

1.1 Solitons

A solitary wave occurs as a localized, non-dispersive and non-singular solution of a non-linear equation, for which superposition principle is not valid. For these waves to exist the balance between nonlinearity and dispersion plays the key role.

It was first discussed in 1845 by J. Scott Russell in the "Report of the British Association for the Advancement of Science", when he observed a solitary wave travelling along a water channel. In his own words, *"I was observing the motion of a boat which was rapidly drawn along a narrow channel by a pair of horses, when the boat suddenly-not so the mass of water in the channel which it had put in motion; it accumulated round the prow of the vessel in a state of violent agitation, then suddenly leaving it behind rolled forward with great velocity, assuming the form of a large solitary elevation, a rounded, smooth and well-defined heap of water, which continued its course along the channel apparently without change of form or diminution of speed. I followed it on horseback, and overtook it still rolling on at a rate of some eight or nine miles an hour, preserving its original figure some thirty feet long and a foot to a foot and a half in height. Its height gradually diminished, and after a chase of one or two miles I lost it in the windings of the channel. Such, in the month of August* 1834, *was my first chance interview with that singular and beautiful phenomenon which I have called the Wave of Translation,...."*

In physical context, nonlinearity arises in the response of the system. When the output response of a system (R) is proportional to the input excitation (E), the

system is a linear one. On the other hand, if the response of the medium:

$$\begin{aligned} R &= a_1E + a_2E^2 + a_3E^3 + ... \\ &= a_1E\left(1 + \frac{a_2}{a_1}E + \frac{a_3}{a_1}E^2 + ...\right), \end{aligned} \tag{1.1}$$

system is called a nonlinear medium. Nonlinearity increases if the ratios $\frac{a_2}{a_1}$, $\frac{a_3}{a_1}$.... are large. It can result in generation of harmonics. In other nonlinear systems points of large amplitude can overtake points of small amplitudes.

Now, let us consider waves, which are time and space dependent. In this case any arbitrary pulse can be regarded as a linear superposition of sinusoidal wave trains with different frequencies. If each of these waves propagates with the same velocity, the system is non-dispersive and the pulse travels without deforming its shape. On the contrary, different velocities for different component waves, results in spreading and the system is a dispersive one. In this case refractive index or the wave vector is a function of the wavelength or the frequency. In optics language, '$\frac{dn}{d\lambda} < 0$' is the normal dispersion '$\frac{dn}{d\lambda} > 0$' is the anomalous dispersion. The group velocity dispersion is characterized by ($\frac{d^2n}{d\lambda^2}$):

$$\begin{aligned} \frac{\lambda}{c}\left(\frac{d^2n}{d\lambda^2}\right) \quad &> 0 \rightarrow \text{positive dispersion} \\ &< 0 \rightarrow \text{negative dispersion,} \end{aligned} \tag{1.2}$$

Solitons are solutions of nonlinear equations, governing different nonlinear media. In recent years one finds a host of research works, where a number of different approaches for finding exact solutions of nonlinear differential equations have been proposed [9, 10, 11, 12, 13, 14, 15, 16, 17]. It is well known that all nonlinear differential equations can be divided into three types: exactly solvable, partially solvable and those that have no exact solution.

Consider the nonlinear evolution equation, whole solution needs to be found:

$$E_1[u] \equiv E_1(u, u_t, u_x, ...x.t) = 0 \tag{1.3}$$

First of all one performs the Painlevé test to check the integrability of this equation [18]. Usually we look for exact solution of nonlinear evolution equation in the form of traveling wave:

$$u(x,t) = y(z), \quad z = x - ut \tag{1.4}$$

As a result, Eq. (1.3) reduces to the nonlinear ordinary differential equation (ODE)

$$E_2[y] \equiv E_2(y, y_z, ..., z) = 0 \tag{1.5}$$

To obtain exact solutions of Eq. (1.5) one can apply different approaches [9, 10, 19, 20, 21, 22, 23, 24, 25, 26, 27, 28]. However, one notes that most methods of exact solutions take into account the singular analysis for solutions of the nonlinear differential equations [18, 19, 20, 29, 30, 31]. In a number of cases, elliptic functions are general solutions of nonlinear exactly solvable equations. It was shown by Zakharov that the time evolution of the envelope of a weakly nonlinear deep-water wave train is described by an equation called the nonlinear Schrödinger equation. Furthermore, this equation was solved exactly by Zakharov and Shabat (1971) by using the inverse-scattering method. They showed that the exact solutions are deep-water wave-*envelope solitons* and that an initial wave packet eventually evolves into a number of envelope solitons and a dispersive tail. These solutions were verified experimentally by Yuen and Lake (1975). In the case of deep water, an envelope soliton consists of a sech-shaped hyperbolic secant envelope which modulates a periodic (cosine) wave. Hasegawa and Tappert (1973) showed theoretically that the envelope of a light wave propagating in an optical fiber can be described by the NLS equation. As a result, the existence of optical-envelope solitons, the so called *bright solitons*, was predicted. This prediction was verified in (1980) by Mollenauer et. al., who observed bright-soliton propagation in a single fiber. Physically, these optical solitons originate from a Kerr type nonlinearity, manifested through the intensity dependence of the refractive index.

Bose-Einstein condensate, is one of the very well-studied nonlinear systems, where nonlinearity arises because of interactions between the bosonic atoms. Optical fibre and non-resonant atomic media are the other systems, with which will be concerned with.

1.2 Bose-Einstein condensates

Bose statistics dates back to a 1924 paper, in which Satyendranath Bose used a statistical argument of photon to derive the black body photon spectrum. Einstein

then extended the idea of Bose's counting statistics to the case of non-interacting atoms. Einstein immediately noticed a peculiar feature of the distribution of the atoms over the quantized energy levels predicted by this statistics. At very low but finite temperature a large fraction of the atoms would go into the lowest energy quantum state.

In his words *"A separation is effected: one part condenses, the rest remains a saturated ideal gas"* [32]. This phenomenon is known as Bose–Einstein condensation (BEC). Particles, which obey Bose–Einstein distribution, are called bosons, for which the distribution function is given by,

$$f(\epsilon) = \frac{1}{e^{(\epsilon-\mu)}/kT - 1}. \tag{1.6}$$

Here, $e^{\mu/KT}$ is called fugacity ($0 \leq e^{\mu/Kt} \leq 1$). At the high temperature limit particles are distributed over a wide energy range and the distribution function goes to the one of Maxwell–Boltzmann classical distribution. On the other hand, at low temperature limit ($< T_c$), the chemical potential (μ) is almost equal to the lowest energy value. In this case, number of particles in single particle ground state becomes arbitrarily large, leading to a macroscopic occupation of a single quantum state or the Bose–Einstein condensation.

This occurs for identical bosons when the inter-particle separation is less than the thermal de Broglie wavelength of the particles: $\lambda_{dB} = h/\sqrt{2\pi m k_B T}$. Here, h, k_B, m, and T are the Planck constant, Boltzmann constant, atomic mass, and temperature of the gas, respectively. For a room temperature gas, λ_{dB} is much less than the size of an atom, hence although λ_{dB} increases for lower temperature, conventional condensation to liquid or solid occurs long before reaching the quantum degenerate regime. Hence, an atomic BEC is a supercooled metastable state that exists in an ultrahigh vacuum chamber, and depending on the vacuum condition, the lifetime of a condensate ranges from only few seconds to few minutes. To prevent formation of normal condensed states, which occur via three-body collisions leading to molecule formation, atoms must be kept at low densities, typically of the order of 10^{14} cm^{-3}, which is 5 orders of magnitude lower than ambient air pressure. At such low densities, atoms need to be cooled to the sub-micro Kelvin regime in order to observe Bose-Einstein condensation. Bose-

Einstein condensates are of purely quantum origin. Quantum effects arise when the gas parameter, $n\lambda^3 \to 1$, where n and λ are the density and the wavelength respectively. The transition temperature (T_c) is the highest temperature at which a macroscopic occupation of lowest-energy state appears.

This can be calculated as [1],

$$k_B T_c = \frac{N^{1/\alpha}}{[C_\alpha \Gamma(\alpha)\zeta(\alpha)]^{1/\alpha}}, \tag{1.7}$$

where N is the total number of atoms and $\zeta(\alpha)$ is the Riemann zeta function: $\zeta(\alpha) = \sum_{n=1}^{\infty} n^{-\alpha}$. For a gas in a 3D box of volume V, $\alpha = 3/2$, $\zeta(3/2) = 2.612$ and $C_{3/2} = \frac{Vm^{3/2}}{\sqrt{2}\pi^2\hbar^3}$. Therefore the transition temperature:

$$k_B T_c = 3.31 \frac{\hbar^2 n^{2/3}}{m} \quad \text{where} \quad n = \frac{N}{V}. \tag{1.8}$$

For 3D harmonic oscillator trap $\alpha = 3$. Condensate fraction is given by

$$N_0 = N[1 - \left(\frac{T}{T_c}\right)^{\alpha}], \tag{1.9}$$

where N_0 is the number of atoms in ground state. At absolute zero ($T = 0$), $N_0 = N$, hence all the atoms are in the ground state.

Experimental realization of BEC started from liquid helium. In 1938 Fritz London, noting the similarity of the heat capacity curve in liquid helium to the behavior of the heat capacity of an ideal gas near the BEC transition, proposed that superfluidity could be a manifestation of Bose-Einstein condensation [33]. This proposal, and its later verification, constitutes a landmark in modern physics. For the very first time a system had been discovered which was described by a macroscopic wave function. Due to the presence of strong interaction in liquid helium, the number of atoms in the zero momentum states was very small, that created the difficulty to realize it in experiments. In 1959, Bose-Einstein condensation in weakly-interacting spin-polarized hydrogen was proposed by Hecht [34]. The attraction between hydrogen atoms is small and it remains gaseous at very low temperature. In the mean time, laser cooling and trapping techniques had been developed, but laser cooling was not feasible for hydrogen.

These problems led to the search for weakly interacting Bose gas with higher condensate fraction. Since then alkali gases have become a strong candidate for

BEC. They remain gaseous at very low temperatures. Alkali atoms are also well suited to laser based methods because their optical transitions can be effected by available laser. They have a favorable internal energy-level structure for cooling to very low temperature.

By combining laser cooling with the evaporative cooling technique BEC in dilute alkali gases had been achieved in 1995 [35, 36, 37]. Since then, many experiments have been performed probing the static and dynamic properties of weakly interacting Bose condensates, and dilute gas BEC has been produced by many experimental groups. Multi-component condensates have been studied by trapping atoms in two different hyperfine states [38]. Multi-component spinor condensates have also been studied [39].

1.3 Gross-Pitaevskii equation

Dynamics of BEC is governed by the time dependent Gross-Pitaevskii (GP) equation. The cubic nonlinearity arises because of two-body atom-atom interactions. We describe the system of N interacting bosons, using the second quantized Hamiltonian in terms of the Bose field operator $\hat{\Psi}$. This operator is a function of space and time, although for convenience one drops the time parameter. The second quantized Hamiltonian is then given by,

$$\hat{H} = \int d^3\mathbf{r}\hat{\Psi}^\dagger(\mathbf{r})H_0\hat{\Psi} + \frac{1}{2}\int d^3\mathbf{r}\int d^3\mathbf{r}'\hat{\Psi}^\dagger(\mathbf{r})\hat{\Psi}^\dagger(\mathbf{r}')V_{int}(\mathbf{r},\mathbf{r}')\hat{\Psi}(\mathbf{r}), \tag{1.10}$$

where $V_{int}(\mathbf{r},\mathbf{r}')$ is the interaction potential acting between the bosons and $H_0 = -(\hbar^2/2m)\nabla^2 + V_{ext}$ is the single particle Hamiltonian, where m is the particle mass and V_{ext} is the external potential acting on the system. The operators $\hat{\Psi}^\dagger(\mathbf{r})$ and $\hat{\Psi}(\mathbf{r})$ represent the creation and annihilation of a boson at position $\mathbf{r}$, and satisfy the crucial Bose commutation rules that will be given below.

The gas is sufficiently dilute that the atomic interaction are dominated by low energy, two-body s-wave collisions. These are essentially elastic, hard-sphere collision between two atoms, and can be modeled in terms of the pseudo-potential,

$$V_{int}(\mathbf{r},\mathbf{r}') = g\delta(\mathbf{r}'-\mathbf{r}), \tag{1.11}$$

where $g = 4\pi\hbar^2 a/m$, with a the s-wave scattering length. Inserting this potential into Eq. (1.10) and integrating over all $\mathbf{r}'$-space leads to,

$$\hat{H} = \int d^3\mathbf{r}\hat{\Psi}^\dagger(\mathbf{r})\hat{H}_0\hat{\Psi} + \frac{g}{2}\int d^3\mathbf{r}'\hat{\Psi}^\dagger(\mathbf{r})\hat{\Psi}^\dagger(\mathbf{r})\hat{\Psi}(\mathbf{r})\hat{\Psi}(\mathbf{r}). \tag{1.12}$$

Using the Bose commutation relations,

$$\left[\hat{\Psi}(\mathbf{r}'),\hat{\Psi}^\dagger(\mathbf{r})\right] = \delta(\mathbf{r}'-\mathbf{r}), \quad \left[\hat{\Psi}(\mathbf{r}'),\hat{\Psi}(\mathbf{r})\right] = \left[\hat{\Psi}^\dagger(\mathbf{r}'),\hat{\Psi}^\dagger(\mathbf{r})\right] = 0, \tag{1.13}$$

Heisenberg's time evolution equation yeilds,

$$\begin{aligned} i\hbar\frac{\partial\hat{\Psi}(\mathbf{r}')}{\partial t} &= \left[\hat{\Psi}(\mathbf{r}'),\hat{H}\right] \\ &= \Psi(\mathbf{r}')\hat{H} - \int d^3\left[\hat{\Psi}(\mathbf{r}')\hat{\Psi}^\dagger(\mathbf{r}) - \delta(\mathbf{r}'-\mathbf{r})\right]\hat{H}_0\hat{\Psi}(\mathbf{r}) \\ &- \frac{g}{2}\int d^3\mathbf{r}\left[\hat{\Psi}(\mathbf{r}')\hat{\Psi}^\dagger(\mathbf{r}) - 2\delta(\mathbf{r}'-\mathbf{r})\right]\hat{\Psi}^\dagger(\mathbf{r})\hat{\Psi}^\dagger(\mathbf{r})\hat{\Psi}^\dagger(\mathbf{r}) \\ &= \left[\hat{H}_0 + g\hat{\Psi}^\dagger(\mathbf{r}')\hat{\Psi}(\mathbf{r}')\right]\hat{\Psi}(\mathbf{r}'). \end{aligned} \tag{1.14}$$

Since the condensate state involves the macroscopic occupation of a single state it is appropriate to decompose the Bose field operator in terms of a macroscopically-populated mean field term $\hat{\psi}(\mathbf{r}') \equiv < \hat{\Psi}(\mathbf{r}') >$ and a fluctuation term $\hat{\Psi}'(\mathbf{r}')$,

$$\hat{\Psi}(\mathbf{r}') = \psi(\mathbf{r}') + \hat{\Psi}'(\mathbf{r}'). \tag{1.15}$$

Then, taking only the leading order terms in ψ, Eq. (1.14) leads to the time-dependent Gross-Pitaevskii equation,

$$i\hbar\frac{\partial\psi}{\partial t} = \left(-\frac{\hbar^2}{2m}\nabla^2 + V_{ext} + g|\psi|^2\right)\psi. \tag{1.16}$$

Here, $\psi \equiv \psi(\mathbf{r},t)$ represents a function of space and time, called the order parameter of the condansate. Neglecting lower order terms involving the fluctuation operator $\hat{\Psi}'$ amounts to neglecting thermal and quantum depletion of the condensate. This is a valid approximation, when (i) the temperature is much less than the transition temperature for the onset of condensation, and (ii) when the condensate is sufficiently weakly-interacting, which is true when $a \ll \lambda_{dB}$, where λ_{dB} is the thermal de Broglie wavelength of the particles.

In this thesis, we shall study the various modification of the GP equation. We mainly concentrate on the quasi-1D scenario. In this case, the transverse

dimensions of the cloud are very small compared to longitudinal direction (z). The density profile across the trap can be assumed to have its equilibrium form, appropriate to the local number of particles per unit length:

$$\sigma(z) = \int n(x, y, z)dxdy. \tag{1.17}$$

With these consideration the system becomes essentially one dimensional [3]. Atom-atom interactions play very important role in the dynamics of BEC. For strong interaction, kinetic energy term becomes small and the nonlinearity and potential dominate. This is known as Thomas-Fermi approximation.

Three-body atom-atom interactions becomes significant for high density and large scattering length. This situation is described by the quintic nonlinear term. Various types of traps are incorporated starting from regular oscillator to an expulsive one. The response of BEC profile, when parameters like, nonlinearity, trap-frequency and phenomenological loss term are time dependent is quite interesting. We have analytically tackled a variety of these systems in realistic conditions.

References

[1] C. J. Pethik, and H. Smith, *Bose-Einstein Condensation in Dilute Gases* (Cambridge University Press, Cambridge, 2002).

[2] G. P. Agrawal, *Nonlinear Fiber Optics* (Academic Press, USA, 2001).

[3] A. D. Jackson, and G. M. Kavoulakis, Phys. Rev. Lett. **89**, 070403 (2002).

[4] M. Ögren and G. M. Kavoulakis and A. D. Jackson, Phys. Rev. A **72**, 021603(R) (2005).

[5] N. Guruppa and P. K. panigrahi Phys. Rev. B **62**, 1943 (2000).

[6] Utpal Roy, J. Banerji and P. K. Panigrahi, J. Phys. A: Math. Gen. **38**, 9115 (2005).

[7] D. J. Kaup and A. C. Newell, Phys. Rev. B **18**, 5162 (1978).

[8] T. S. Raju, C.N. Kumar, and P. K. Panigrahi, J. Phys. A: Math. Gen. **38**, L271 (2005).

[9] M. Musette and R. Conte, Physics D **181**, 70-79 (2003).

[10] S. K. Liu, Z. T. Fu, S. D. Liu *et al.*, Phys. Lett. A **309**, 234 (2003).

[11] Z. Y. Yan, Chaos Solitons Fractals, **15**, 575 (2003).

[12] Z. Y. Yan, Chaos Solitons Fractals, **15**, 891 (2003).

[13] S. A. Elwaskil, S. K. Ellabany, M. A. Zahran *et al.*, Phys. Lett. A **299**, 179 (2002).

[14] E. G. Fan, Nuovo Cimento B **116**, 1385 (2001).

[15] Z. T. Fu, S. K. Liu, S. D. Liu *et al.*, Phys. Lett. A **290**, 72 (2001).

[16] E. G. Fan and L. Chao, Phys. Lett. A **285**, 373 (2001).

[17] N. A. Kudryashov, M. B. Soukharev, J. Appl. Math. Mech **65**, 855 (2001).

[18] R. Conte (ed) 1999, The Painleve approach of nonlinear ordinary differential equations *The Painleve Property. One Century Later (CRM Series in Mathematics Physics)* (Berlin: Springer).

[19] N. A. Kudryashov, Journal of Applied Mathematics and Mekhanics, **52**, 361-365 (1988)

[20] R. Conte and M. Musette, J. Phys. A **22**, 169-177 (1989).

[21] N. A. Kudryashov, Phys Lett. A **147**, 287-291 (1990).

[22] N. A. Kudryashov, Phys Lett. A **155**, 269-275 (1991).

[23] N. G. Berloff, L. N. Howard, Stud. Appl. Math **99**, 1-24 (1997).

[24] N. G. Berloff, L. N. Howard, Stud. Appl. Math **100**, 195-213 (1998).

[25] N. A. Kudryashov., Analytical theary of nonlinear diffeential equations, Moscow-Igevsk, IKI (2003).

[26] S. R. Choudhury, Phys. Lett. A, **159**, 311-317 (1997).

[27] R. Conte, M. Musete, J. Phys. A: Math. Gen. **25**, 5609-5623 (1992).

[28] N. A. Kudryashov and E. D. Zargaryan, J. Phys. A: Math. and Gen **29**, 8067-8077 (1996).

[29] F. L. Ince, *Ordinary Differential Equations*, (Dover, New York, 1956).

[30] J. Weiss, M. Tabor and G. Carnevalle, J. Math. Phys **24**, 522-526 (1983).

[31] A. Pickering, J. Phys. A: Math. Gen., **26**, 288-300 (1993).

[32] A. Einstein, Sitzungsber. Preuss. Akad. Wiss., Bericht **3**, 18 (1925).

[33] F. London, Nature **141**, 643 (1938).

[34] Charles E. Hecht, Physica **25**, 1159 (1959).

[35] M. H. Anderson, J. R. Ensher, M. R. Matthews, C. E. Wieman, and E. A. Cornell, Science **269**, 198 (1995).

[36] K. B. Davis, M.-O. Mewes, M. R. Andrews, N. J. van Druten, D. S. Durfee, D. M. Kurn, and W. Ketterle, Phys. Rev. Lett **75** 3969 (1995).

[37] C. C. Bradley, C. A. Sackett, and R. G. Hulet, Phys. Rev. Lett **78** 985 (1997).

[38] D. S. Hall, M. R. Matthews, J. R. Ensher, C. E. Wieman, and E. A. Cornell, Phys. Rev. Lett **81** 4531 (1998).

[39] J. Stenger, S. Inouye, D.M. Stamper-Kurn, H.-J. Miesner, A.P. Chikkatur, and W. Ketterle, Nature **396** 345 (1998).

Chapter 2

Coherent control of solitons in strongly coupled cigar-shaped BEC

We find exact localized solutions of strongly coupled Bose-Einstein condensate (BEC) in a one-dimensional harmonic trap and illustrate the procedure for their coherent control. These solitons of the repulsive BEC exhibit a W type density distribution, well suited for trapping of neutral atoms. We demonstrate the effect of time dependencies of the coupling, trap potential and loss on the condensate profile. The dynamical stability of the solutions is checked, using the spectral method. An interesting correspondence is established between these solutions and the complex Lieb-mode of weakly coupled BEC.

2.1 Introduction

The formation dynamics and control of the non-linear waves in Bose-Einstein condensate (BEC) are subjects of intense current research [1, 2, 3, 4, 5, 6, 7]. Dark [8] and bright solitons [9, 10, 11, 12] and soliton trains [13] have been experimentally observed in cigar shaped BEC, although the precise mechanism of their formation still remains unclear. The fact that in the weak coupling limit, the 1D Gross-Pitaevskii (GP) equation is the familiar non-linear Schrödinger equation (NLSE) with a well-studied cubic non-linearity [14], has tremendously facilitated our understanding of the structure of this macroscopic quantum system. The above system, being integrable, the solutions are well known since long time.

Recently, the coherent control of the weakly coupled BEC and the behavior of the solitons in a harmonic trap with time dependent scattering length are being extensively studied [15, 16, 17, 18, 19]. In cigar shaped BEC, apart from time dependent scattering length arising through Feshbach resonance, one can also analytically tackle various time dependencies of oscillator frequency, both in attractive and repulsive scenarios. This has found important application in the generation of Faraday waves in BEC [20], which arise due to sinusoidal temporal modulation of the transverse trap/scattering length.

In comparison to the weak coupling regime, the strongly coupled sector has not been studied carefully. Lack of exact solutions has led to primarily numerical investigations and variational approaches to the Thomas-Fermi limit [21, 22, 23] of the GP equation [24, 25, 26]. Goal of the present work is two-fold. First of all, we present a method to obtain exact solutions of the strongly coupled GP equation in a cigar shaped trap. Localized singular and non-singular solutions as well as periodic ones emerge from the above procedure. The localized solution in the repulsive regime exhibits a W type density profile. This solution is found to be dynamically stable through the use of a spectral method. W type density profile of the soliton is well suited for trapping of neutral atoms.

We then study the coherent control of these solutions in the presence of a harmonic trap, which can be confining or expulsive. Time dependent non-linearity and loss have been treated exactly. In this case, the self-similar solutions get modified with time dependent amplitude, phase and width. The center of mass of the solitons reveals rich dynamics, which for a regular confining oscillator is periodic. Interestingly, we establish a connection of these solutions with the complex Lieb mode of weakly coupled BEC [25].

The chapter is organized as follows. In Sec.2.2, we first outline the procedure to obtain the GP equation in one dimension, after which a method of fractional transform is used to find a wide class of exact solutions. The non-singular localized solutions and the singular ones are isolated in the repulsive domain. The connection of these solutions, with the Lieb-mode for weakly coupled BEC is then established. Subsequently in Sec.2.3, their coherent control is analytically demonstrated in presence of an oscillator. Stability analysis of the solutions is

carried out in Sec. 2.4.

2.2 Exact solitons of the strongly coupled BEC

The three dimensional GP equation describing the dynamics of BEC in a cylindrical harmonic trap, $V = \frac{1}{2}M\omega_\perp^2(x^2+y^2)$, is given by

$$i\hbar\frac{\partial\Psi(\mathbf{r},t)}{\partial t} = \left[-\frac{\hbar^2}{2M}\nabla^2 + U_0|\Psi(\mathbf{r},t)|^2 + V\right]\Psi(\mathbf{r},t), \tag{2.1}$$

where $U_0 = 4\pi\hbar^2 a/M$ is the contribution from the effective two body interaction, a being the scattering length. In the quasi-one dimensional limit, one writes [25]

$$\Psi(\mathbf{r},t) = f(z,t)G(x,y,\sigma), \tag{2.2}$$

where $\sigma(z)$ is the local particle density. $G(x,y,\sigma)$ is the normalized equilibrium wave function for the transverse motion:

$$\sigma(z) = \int dxdy|\Psi(x,y,z)|^2 = |f(z,t)|^2. \tag{2.3}$$

We first assume that there is no confinement along the z direction. In the repulsive, strong coupling limit ($n_0U_0 >> \hbar\omega_\perp$), one uses the Thomas-Fermi approximation for the transverse profile, leading to the condensate equation [24],

$$i\hbar\frac{\partial}{\partial t}f(z,t) = \left[-\frac{\hbar^2}{2M}\frac{\partial^2}{\partial z^2} + 2\hbar\omega_\perp a^{1/2}(\sigma^{1/2} - \sigma_0^{1/2})\right]f(z,t). \tag{2.4}$$

Here, σ_0 is the equilibrium density of the atoms far away from the axis. For finding exact solutions, we consider the following ansatz solution

$$f(z,t) = e^{i(kz-\omega t)}\rho(\xi), \tag{2.5}$$

with a fast moving component and slowly varying envelope profile $\rho(\xi)$. Here, $\xi = \alpha(z-vt)$ and $v = \frac{\hbar}{M}k$. Real $\rho(\xi)$ satisfies,

$$\alpha^2\rho'' + g\rho^2 + \epsilon\rho = 0, \tag{2.6}$$

where $g = -4M\omega_\perp a^{1/2}/\hbar$ and $\epsilon = 2M\omega/\hbar + 4M\omega_\perp(\sigma_0 a)^{1/2}/\hbar - k^2$. In the repulsive domain under consideration, g is always negative. Following a pseudo potential picture, one obtains the constant of motion as,

$$E_0 = \frac{\alpha^2}{2}\rho'^2 + g/3\ \rho^3 + \epsilon/2\ \rho^2. \tag{2.7}$$

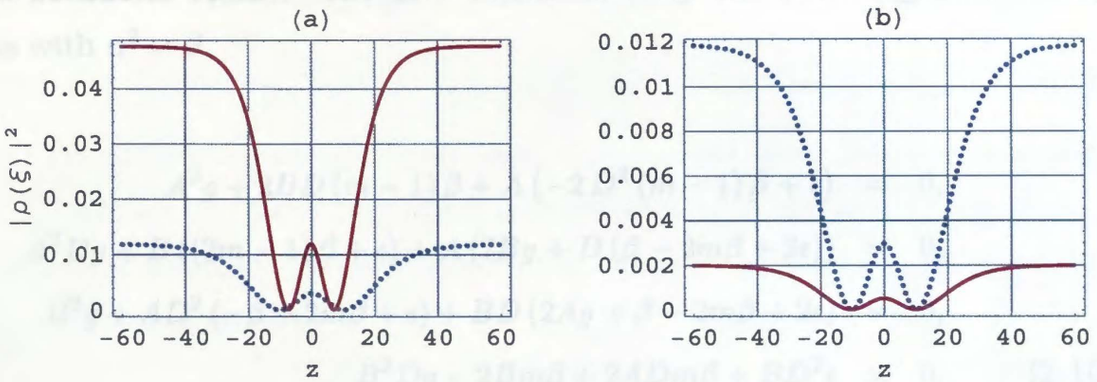

Figure 2.1: Localized soliton with a double well density profile for an atomic BEC of mass $M = M_{Na}$ with (a) $\omega = 2.8$ (blue/dotted line) and $\omega = 28$ (red/solid line) and (b) scattering length 189 *a.u.* (blue/dotted line) and 1134 *a.u.* (red/solid line). ω is in the unit of 10^{-9}*a.u.*.

The energy E_0, being cubic in ρ indicates the possibility of a W type density profile. For example, for $E_0 = 0$, $\rho(\xi) = 0$ and $\rho(\xi) \neq 0$ are possible extrema solutions. For obtaining exact solutions, we use a rational ansatz [27]:

$$\rho(\xi) = \frac{\sum a_n f^n}{1 + \sum a_n f^n}. \tag{2.8}$$

It needs to be ensured that this fractional transform connects the solution $\rho(\xi)$ to elliptic equation: $f'' = af - bf^3$. Here $f(\xi)$ is one of the 12 Jacobian elliptic functions [28]. This procedure gives both singular and non-singular solutions, as will be soon seen. The maximum power is found to be, $n = 2$, with the general solution:

$$\rho(\xi) = \frac{A + B\, f(\xi) + C\, f^2(\xi)}{1 + D\, f(\xi) + F\, f^2(\xi)}. \tag{2.9}$$

For the sake of explicitness, we consider the solutions of the above type, with $f = cn(\xi, m)$, m being the modulus parameter ($0 \leq m \leq 1$). We note that $cn(\xi, 0) = cos(\xi)$ and $cn(\xi, 1) = sech(\xi)$. The latter one leads to localized solutions. A, B, C, D and F are real parameters to be determined from the consistency conditions arising from Eq. 3.6. It can be seen that these conditions are seven in number, indicating the constrained nature of the general solution. The solutions are unconstrained when two of the parameters vanish. Two particularly interesting configurations correspond to $C = F = 0$, *i.e.*, linear fractional transform (LFT) and $B = D = 0$, *i.e.*, quadratic fractional transform (QFT). For $AD - B = 0$ or $AF - C = 0$, constant

amplitude solutions result. The LFT solutions obey the following consistency conditions with $\alpha^2 = \beta$,

$$\begin{aligned} A^2 g + 2BD\,(m-1)\,\beta + A\left(-2\,D^2\,(m-1)\,\beta + \epsilon\right) &= 0, \\ A^2 Dg + B\left((2m-1)\,\beta + \epsilon\right) + A\left(2Bg + D\left(\beta - 2m\beta + 2\epsilon\right)\right) &= 0, \\ B^2 g + AD^2\left(-\beta + 2m\beta + \epsilon\right) + BD\left(2Ag + \beta - 2m\beta + 2\epsilon\right) &= 0, \\ B^2 Dg - 2Bm\beta + 2ADm\beta + BD^2\epsilon &= 0. \end{aligned} \tag{2.10}$$

In the following, we concentrate on the localized solutions because of its physical interest:

$$\rho(\xi) = -\frac{\epsilon}{g}\left(\frac{1 - 2sech(\xi)}{1 + sech(\xi)}\right); \tag{2.11}$$

the width is found to be $\alpha = \epsilon^{1/2}$. This solution exists in the repulsive domain in the static limit, or when $\omega = \frac{\hbar k^2}{2m}$. The width and the amplitude of the solutions are coupled. Interestingly, the above solution can be cast in an alternate form,

$$\rho(\xi) = \frac{A + B'\,sech^2\xi/2}{1 + D'\,sech^2\xi/2}, \tag{2.12}$$

where $B' = \frac{1}{2}(B - A)$ and $D' = \frac{1}{2}(D - 1)$. Thus for $D = 1$, as is the case in Eq. 2.11, localized fractional transform solution gives rise to a linear expression [26]:

$$\rho(\xi) = -\frac{\epsilon}{g}\left(1 - \frac{3}{2}sech^2(\xi/2)\right). \tag{2.13}$$

This dark soliton has a W type density profile as is seen in Fig. 2.1. The two points where the order parameter vanishes, may be useful for trapping of neutral atoms. As will be shown later, the barrier height and the locations of minima can be controlled, by changing the frequency and the scattering length, which can be manipulated through Feshbach resonance [29, 30]. With the increase in the value of frequency ω, the two wells come closer and the barrier height and the background density become larger (Fig. 2.1(a)). Larger values of scattering length a makes the double-well flatter, which is seen in Fig. 2.1(b). The fact that these minima locations can be controlled including the barrier height, makes these solutions potentially attractive for quantum computation purpose. One can also

have cnoidal wave solutions ($m = \frac{1}{2}$):

$$\rho(\xi) = \frac{\epsilon}{2g}\left(\frac{-1+\sqrt{3}-(1+\sqrt{3})cn^2(\xi,1/2)}{1+cn^2(\xi,1/2)}\right), \tag{2.14}$$

where $\beta = \frac{\epsilon}{2\sqrt{3}}$. It is interesting to note that, the cnoidal wave solution is a non-singular member for the quadratic fractional transform. When $m = 1$, one finds a singular localized solution. We now analyze the singular solutions more carefully. For LFT of $m = 1$, it is given by

$$\rho(\xi) = -\frac{\epsilon}{g}\left(\frac{1+2sech(\xi)}{1-sech(\xi)}\right). \tag{2.15}$$

Here, $\alpha = \sqrt{\epsilon}$. Localized QFT-solution for $m = 1$ and $\beta = \epsilon/4$, is also singular in nature:

$$\rho(\xi) = -\frac{\epsilon}{2g}\left(\frac{2+sech^2(\xi)}{1-sech^2(\xi)}\right), \tag{2.16}$$

which can be cast in the alternate form, as a combination of singular and non-singular solutions:

$$\rho(\xi) = -\frac{\epsilon}{4g}\left[\frac{1}{1-sech(\xi)}+\frac{1}{1+sech(\xi)}\right](2+sech^2(\xi)). \tag{2.17}$$

Oscillatory ($m = 0$) solutions are obtained for $B = 0$ and $\beta = \epsilon$:

$$\rho(\xi) = -\frac{3\epsilon}{g}\left(\frac{1}{1\pm cos(\xi)}\right). \tag{2.18}$$

These are singular and of mono frequency. Singular solutions indicate resonant increase in BEC density, exhibiting self-focussing of atoms at certain point. These are analogous to the self-focussing effect in optical fibers and hollow-core wave guides [31]. For completeness, we also studied the solutions for LFT with $f(\xi) = sn(\xi,m)$ and $dn(\xi,m)$. The consistency conditions for the solutions, with $m = 0$, for the first case is found to be the same, as that for $cn(\xi,m)$. There is no solution for $m = 1$. In case of QFT, the solutions for other functions can be obtained by using the relations between different elliptic functions: $dn^2(\xi,m) = 1 - msn^2(\xi,m)$ and $sn^2(\xi,m) = 1 - cn^2(\xi,m)$.

2.2.1 Connection between Lieb-mode of weakly coupled BEC and soliton in the Thomas-Fermi sector

The soliton solution found here is quadratic in the power of $sech(x)$. It is well known that the fundamental soliton in the NLSE is linear in $sech(x)$ and $tanh(x)$.

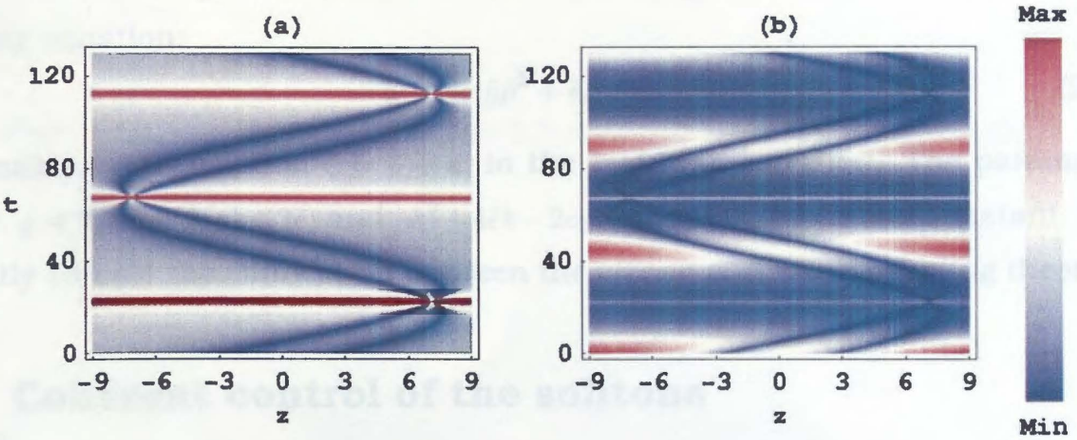

Figure 2.2: Propagation of W type soliton in time (a) without loss for $M_0 = 0.07$, $A_0 = 0.5$, $\lambda = -1$ and $\gamma_0 = 10$ and (b) with loss for $a_1 = -0.5 \times 10^{-3}$, $a_2 = 0.6$ and $\delta = 0.14$.

This indicates the possibility of interconnection between the two dynamical equations. Below, we find a precise connection, which relates the complex Lieb-type solution of weak coupling GP equation, with the localized solution in the strong coupling sector. In the weak coupling regime the condensate equation is given by [24],

$$i\hbar\frac{\partial}{\partial t}\phi(z,t) = \left[-\frac{\hbar^2}{2M}\frac{\partial^2}{\partial z^2} + 2\hbar\omega_\perp a(\tilde{\sigma} - \tilde{\sigma_0})\right]\phi(z,t). \tag{2.19}$$

Here, $|\phi|^2 = \tilde{\sigma}$ and $\tilde{\sigma_0}$ is the equilibrium density. For the ansatz solution

$$\phi(z,t) = e^{i(\chi(\xi)-\omega t)}\tilde{\rho}(\xi), \tag{2.20}$$

real $\tilde{\rho}$ satisfies,

$$\alpha^2\tilde{\rho}'' + \tilde{g}\tilde{\rho}^3 + \tilde{\epsilon}\tilde{\rho} = \frac{c}{\tilde{\rho}^3}. \tag{2.21}$$

Here $g = -4M\omega_\perp a/\hbar$, $\epsilon = \frac{2M}{\hbar^2}\left(\frac{1}{2}Mv^2 + \hbar\omega + 2a\hbar\omega_\perp\tilde{\sigma_0}\right)$ and c is an integration constant. The velocity, phase and amplitude are related as

$$\chi' = \frac{Mv}{\hbar\alpha} + \frac{c}{\tilde{\rho}^2}. \tag{2.22}$$

The once integrated envelope equation (Eq. 2.21), with $\tilde{\rho}^2 = \zeta$ yields,

$$\alpha^2\zeta'^2 + 2g\zeta^3 + 4\epsilon\zeta^2 + 4c_1\zeta = -4c, \tag{2.23}$$

where c_1 is the integration constant. Differentiating once, one obtains the strong coupling equation:

$$\alpha^2\rho'' + \tilde{g}\rho^2 + \tilde{\epsilon}\rho = 0, \tag{2.24}$$

after making a translation $\zeta = \rho + k$, in the resulting equation. The parameters satisfy, $g = 3\tilde{g}$, $\epsilon = 2(gk + 2\tilde{\epsilon})$ and $gk^2 + 4\tilde{\epsilon}k - 2c_1 = 0$, where k is a real constant. This explicitly reveals the connection between the strong and weak coupling theories.

2.3 Coherent control of the solitons

In the following, we analyze the dark solitons in the presence of harmonic confinement with time dependent nonlinearity and loss. The oscillator frequency itself can be time dependent. These distributed coefficients lead to the coherent control of the soliton. It can be compressed and its center of mass can be made to have desired dynamics. For the sake of comparison with the weak coupling case [15], the GP equation is cast in the form

$$i\partial_t\psi = -\frac{1}{2}\partial_{zz}^2\psi + \gamma(t)|\psi|\psi + \frac{1}{2}M(t)z^2\psi + \frac{i\kappa(t)}{2}\psi. \tag{2.25}$$

Here ψ, t and z have been scaled, respectively by $a_B^{1/2}$, $\omega_\perp$ and $1/a_\perp$, making them dimensionless. $\gamma = 2(a(t)/a_B)^{1/2}$ is time dependent non-linearity coefficient, controllable through Feshbach resonance; $M(t) = \omega_0^2(t)/\omega_\perp^2$ is related to the axial trap frequency, which can be made time dependent. $\kappa(t) = \eta(t)/\hbar\omega_\perp$ is time dependent loss term. The oscillator length in the transverse direction is defined as $a_\perp = (\hbar/M\omega_\perp)^{1/2}$ and a_B is the Bohr radius. We consider the following ansatz solution for $\psi(z,t)$,

$$\psi(z,t) = B(t)F(\xi)e^{\left[i\Phi(z,t)+\frac{1}{2}G(t)\right]}, \tag{2.26}$$

where $\xi = A(t)\{z - l(t)\}$, $l(t) = \int_0^t v(t')dt'$ and $G(t) = \int_0^t \kappa(t')dt'$. The phase has been taken in the form $\Phi(z,t) = a(t) + b(t)z - \frac{1}{2}c(t)z^2$, where $a(t)$ is a z independent phase term: $a(t) = a_0 + \frac{\lambda-1}{2}\int_0^t A^2(t')dt'$. The parameter λ characterizing the time dependent phase specifies the energy of different solutions. The solutions are necessarily chirped in time and space, with time varying amplitude and width. $b(t)$ is a time dependent momentum and $c(t)$ balances the oscillator, leading to the

Riccati equation:

$$c_t - c^2(t) = M(t). \tag{2.27}$$

The above can be cast as the familiar Schrödinger eigen value equation:

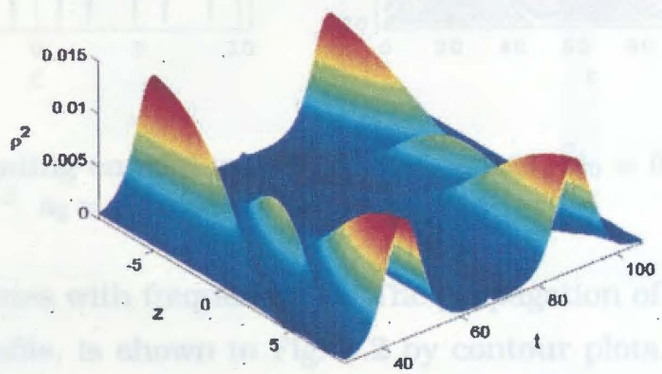

Figure 2.3: 3D plot of the propagation in Fig. 2.2 from $t = 30$ to 107 with the same parameter values.

$$-\phi''(t) - M(t)\phi(t) = 0, \tag{2.28}$$

via a change of variable: $c(t) = -\frac{\partial ln\phi(t)}{\partial t}$. The constant part of $M(t)$ acts as the eigen value. A number of variations in the oscillator frequency can be analytically incorporated from solvable quantum mechanical problems. The oscillator can also be made expulsive. The location of the condensate profile satisfies, $dl(t)/dt + c(t)l(t) = b(t)$. Other parameters are obtained using the following consistency conditions: $B(t) = B_0\ exp(1/2\int_0^t c(t')dt')$, $\gamma(t) = \gamma_0(A(t)/A_0)^{3/2}exp(-G(t)/2)$, and $A(t) = B^2(t) = b(t)$. The real part of the GP equation yields,

$$F''(T) - \frac{2\gamma_0}{{A_0}^{3/2}}F^2(T) - \lambda F(T) = 0, \tag{2.29}$$

which takes the form of Eq. 3.6 with $g = -\frac{2\gamma_0\beta}{{A_0}^{3/2}}$, $\epsilon = -\lambda\beta$ and $T = A(t)[z - l(t)]$. One can find various singular and non-singular solutions for $F(T)$, using the previous procedure, provided g is constant. We now discuss about a number of specific cases of interest.

I. Let us first consider a time independent oscillator frequency with $M(t) = {M_0}^2$. The width and amplitude are determined by the function $A(t)$ which is found to be $A_0 sec(M_0 t)$. The center of the soliton satisfies $l(t) = \frac{A_0}{M_0} sin(M_0 t)$. Thus the center

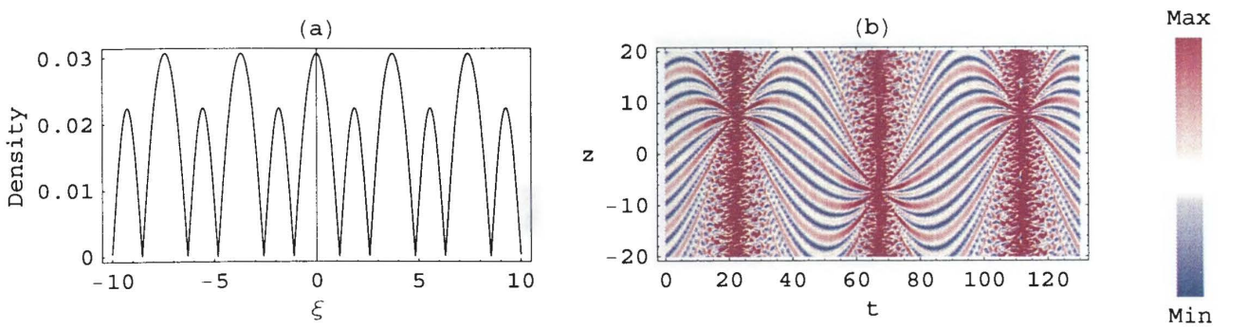

Figure 2.4: Propagating cnoidal waves with $M_0 = 0.07$, $A_0 = 0.5$, $\lambda = -1$, $\gamma_0 = 10$ and $a_1 = -0.5 \times 10^{-3}$, $a_2 = 0.6$ and $\delta = 0.14$.

of the profile oscillates with frequency M_0. The propagation of the dark soliton of W-type density profile, is shown in Fig. 2.2 by contour plots. Fig. 2.2(a) shows the propagation without any loss ($G(t) = 0$). In this case the profile oscillates periodically with period $2\pi/M_0$, associated with a periodic increase in density at intervals $t = \pi/(2M_0)$.

II. In presence of a time dependent loss term: $\kappa(t) = a_1 t - a_2 sin\delta t$, collapse and revival phenomena of the W type dark density profile is depicted in Fig. 2.2(b). This yields $G(t) = a_1/2\ t^2 + a_2/\delta\ (cos\delta t - 1)$. Here $a_1 < 0$ to signify a loss. As time progresses the solution dies down and at times which are multiples of $2\pi/\delta$ the profile reappears. This solution can be written as

$$\psi(z,t) = -\frac{\epsilon}{g}\ \sqrt{A_0 sec(M_0 t)}\ \ [1 - \frac{3}{2} sech^2(T/2)] \times e^{i\Phi(z,t)+\frac{1}{2}G(t)} \tag{2.30}$$

The collapse and revival have been clearly depicted in Fig. 2.3.

III. In presence of oscillator potential the cnoidal waves show interesting dynamical behavior as seen in Fig. 2.4. Individual maxima of the solution oscillate with same frequency, but with different amplitudes. They accumulate and move away in a periodic manner.

IV. We now turn our attention to the dark solution in an expulsive potential ($M(t) = -M_0^2$), where the W type density profile is given by,

$$\psi(z,t) = -\frac{\epsilon}{g}\ \sqrt{A_0 sech(M_0 t)}\ \ [1 - \frac{3}{2} sech^2(T/2)] \times e^{i\Phi(z,t)}. \tag{2.31}$$

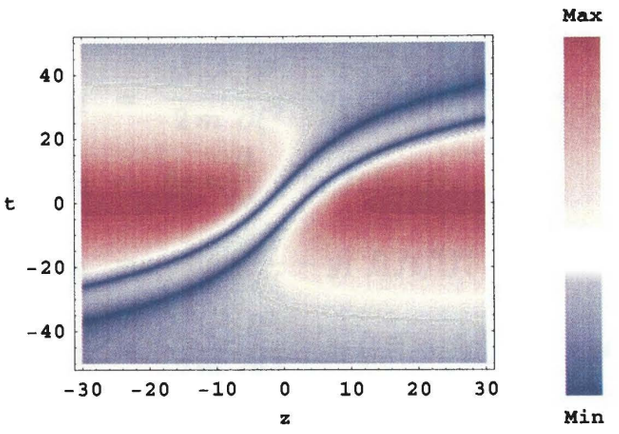

Figure 2.5: Propagation of W type soliton in the expulsive case, without loss. The parameters are same as in Fig. 2.2.

This case is very different from the previous one. Here, $A(t) = A_0 sech(M_0 t)$ and $l(t) = \frac{A_0}{M_0} sinh(M_0 t)$. Thus, the profile has a transient character, as seen in Fig. 2.5. The velocity of center of the soliton increases very rapidly with time.

2.4 Stability of the dark soliton

In this section, we will examine the dynamical stability of obtained solutions. A small perturbation around a stationary solution: $f(z,t) = f(z) + \delta f(z,t)$ is considered. Here, $f = (f_1 + i\, f_2)$ and $\delta f(z,t) = \delta f_1(z,t) + i\, \delta f_2(z,t)$. We separate out the real and imaginary parts of the resulting nonlinear equation. In the Spectral method [32, 33], one writes the perturbation: $\delta f_{1,2} = \delta \bar{f}_{1,2} e^{\lambda t}$, which results in an eigenvalue problem:

$$\mathbf{A}\,\vec{\varphi} = \hbar\lambda\,\mathbf{J}\,\vec{\varphi}. \tag{2.32}$$

$\vec{\varphi}$ is a two-dimensional vector and its components are real and imaginary parts of the perturbation: $\vec{\varphi} = (\delta\bar{f}_1\ \delta\bar{f}_2)^T$. Here, J is a two-dimensional skew-symmetric matrix with $J_{11} = J_{22} = 0$ and $J_{12} = -J_{21} = 1$. The elements of the matrix operator

A are

$$
\begin{aligned}
A_{11} &= \frac{\hbar^2\alpha^2}{2m}\frac{\partial^2}{\partial\xi^2} - g_1\left(|f| + f_1^2/|f|\right) + \mu, \\
A_{12} &= \hbar\alpha\, u\frac{\partial}{\partial\xi} - g_1\, f_1 f_2/|f|, \\
A_{21} &= -\hbar\alpha\, u\frac{\partial}{\partial\xi} - g_1\, f_1 f_2/|f| \quad \text{and} \\
A_{22} &= \frac{\hbar^2\alpha^2}{2m}\frac{\partial^2}{\partial\xi^2} - g_1\left(|f| + {f_2}^2/|f|\right) + \mu,
\end{aligned}
$$

where $\xi = \alpha(z - vt)$, is the traveling coordinate. Nonlinearity coefficient $g_1 = 2\hbar\omega_\perp a^{1/2}$ and $\mu = 2\hbar\omega_\perp(a\sigma_0)^{1/2}$. The soliton solution is stable if real part of the eigenvalue λ is negative or zero. For the real solutions, $f_2 = 0$ and $\delta\bar{f}_1$ is expanded into a spectral series over 900 modes. Our analysis shows that the dark soliton is dynamically stable in a wide parameter range including the experimental ones, used in earlier analysis [25].

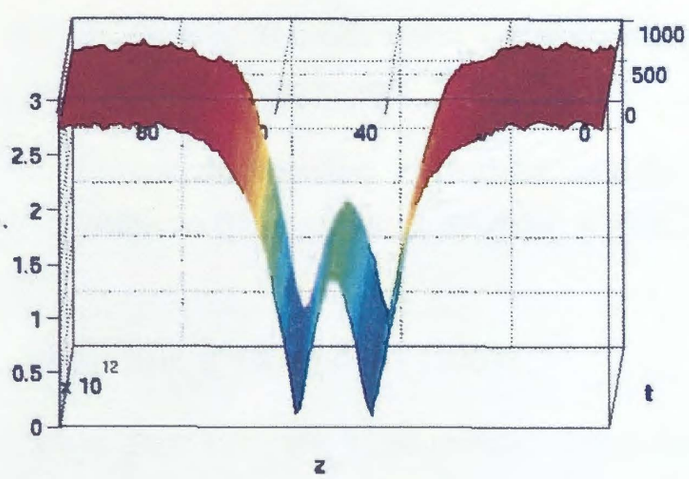

Figure 2.6: Direct numerical evolution of W type soliton with $dz = 0.0003$, $dt = 0.0001$ for 1000 iterations. Parameters are taken as Fig. 2.1(a) dotted graph.

We have also numerically evolved the W-type solution, using the Crank Nicholson finite difference method, which is unconditionally stable. In this analysis, the initial profile has been taken as $\psi(z, t = 0) = \psi(z, t = 0) + \epsilon$, where ϵ is a function, which assumes a random value at each point. The analysis was carried out with $dz = 0.0003$, $dt = 0.0001$ for 1000 cycles. Fig. 2.6 shows that, the W-type soliton remains unchanged except some very small perturbation, where ϵ is taken

10 percent of the peak value of ψ. The minima positions and the width remained unaltered. We have also checked the evolution of the number of particles, which also remains constant.

References

[1] A. J. Leggett, Rev. Mod. Phys. **73**, 307 (2001).

[2] W. Ketterle, Rev. Mod. Phys. **74**, 1131 (2002).

[3] J. R. Anglin, and W. Ketterle, Nature **416**, 211 (2002).

[4] F. Dalfovob, S. Giorgini, L. Pitaevskii, and S. Stringari, Rev. Mod. Phys. **71**, 463 (1999); J. O. Andersen, Rev. Mod. Phys. **76**, 599 (2004); O. Morsch, and M. Oberthaler, Rev. Mod. Phys. **78**, 179 (2006).

[5] C. J. Pethik, and H. Smith, *Bose-Einstein Condensation in Dilute Gases* (Cambridge University Press, Cambridge, 2002).

[6] A. Griesmaier, J. Werner, S. Hensler, J. Stuhler, and T. Pfau, Phys. Rev. Lett. **94**, 160401 (2005); A. Griesmaier, J. Stuhler, and T. Pfau, Appl. Phys. B **82**, 211 (2006).

[7] U. Al Khawaja, Phys. Rev. E **75**, 066607 (2007).

[8] S. Burger *et al.*, Phys. Rev. Lett. **83**, 5198 (1999); J. Denshlag *et al.*, Science **287**, 97 (2000).

[9] U. Al Khawaja, H. T. C. Stoof, R. G. Hulet, K. E. Strecker, and G. B. Partridge, Phys. Rev. Lett. **89**, 200404 (2002).

[10] L. Khaykovich *et al.*, Science **296**, 1290 (2002).

[11] K. E. Strecker *et al.*, New J. Phys. **5**, 73 (2003).

[12] S. L. Cornish, S. T. Thompson, and C. E. Wieman, Phys. Rev. Lett. **96**, 170401 (2006).

[13] K. E. Strecker, G. B. Patridge, A. G. Truscott, and R. G. Hulet, Nature **417**, 150 (2002).

[14] V. E. Zakharov, and A. B. Shabat, Zh. Eksp. Teor. Fiz. **64**, 1627 (1973) [Sov. Phys. JETP **37**, 823 (1973)]; J. R. Taylor, *Optical Solitons: Theory and Experiments* (Cambridge University Press, Cambridge, 1992).

[15] R. Atre, P. K. Panigrahi, and G. S. Agarwal, Phys. Rev. E **73**, 056611 (2006).

[16] Z. X. Liang, Z. D. Zhang, and W. M. Liu, Phys. Rev. Lett. **94**, 050402 (2005).

[17] V. Ramesh Kumar, R. Radha, and P. K. Panigrahi, under consideration for publication in Phys. Rev. A.

[18] R. Atre, and P. K. Panigrahi, accepted for publication in Phys. Rev. A.

[19] U. Al Khawaja, cond-mat/0706.2705.

[20] K. Staliunas, S. Longhi, and G. J. deValcarcel, Phys. Rev. Lett. **89**, 210406 (2002); K. Staliunas, S. Longhi, and G. J. deValcarcel, Phys. Rev. A **70**, 011601(R) (2004); P. Engels, C. Atherton and M. A. Hoefer, Phys. Rev. Lett. **98**, 095301 (2007).

[21] G. Baym, and C. J. Pethick, Phys. Rev. Lett. **76**, 6 (1996).

[22] P. Schuck, and X. Viñas, Phys. Rev. A **61**, 043603 (2000).

[23] A. Munoz Mateo, and V. Delgado, Phys. Rev. A **74**, 065602 (2006).

[24] A. D. Jackson, G. M. Kavoulakis, and C. J. Pethick, Phys. Rev. A **58**, 2417 (1998).

[25] A. D. Jackson, and G. M. Kavoulakis, Phys. Rev. Lett. **89**, 070403 (2002).

[26] L. Salasnich, A. Parola, and L. Reatto, Phys. Rev. A **65**, 043614 (2002).

[27] T. S. Raju, C. N. Kumar, and P. K. Panigrahi, J. Phys. A: Math. Gen. **38**, L271 (2005).

[28] P. F. Byrd, and M. D. Friedman, *Handbook of Elliptic Integrals for Engineers and Physicists* (Berlin-Göttingen-Heidelberg: Springer-Verlag, XIII, 1954).

[29] E. A. Donley, N. R. Claussen, S. L. Cornish, J. L. Roberts, E. A. Cornell, and C. E. Wieman, Nature **412**, 295 (2001); S. Inouye *et al.*, Nature **392**, 151 (1998).

[30] S. B. Papp and C. E. Wieman, Phys. Rev. Lett. **97**, 180404 (2006); C. Yuce, and A. Kilic, Phys. Rev. A **74**, 033609 (2006).

[31] L. F. Mollenauer, R. H. Stolen, and J. P. Gordon, Phys. Rev. Lett. **45**, 1095 (1980); R. W. Boyd, *Non-linear Optics* (MA: Academic, Boston, 1992); G. Fibich, and A. L. Gaeta, Opt. Lett. **25**, 335 (2000).

[32] Y. Y. Su, and B. Khomami, J. Comput. Phys. **100**, 297 (1992).

[33] I. V. Barashenkov, S. R. Woodford, and E. V. Zemlyanaya, Phys. Rev. Lett. **90**, 054103 (2003).

Chapter 3

Complex solitons in Bose-Einstein condensates with two- and three-body interactions

Complex, localized stable solitons, characterized by a power law behaviour, are found for a quasi-one-dimensional Bose-Einstein condensate with two- and three-body interactions. Both dark and bright solitons can be excited in the experimentally allowed parameter domain, when two and three-body interactions are respectively repulsive and attractive. These solutions are obtained for non-zero chemical potential, unlike their unstable real counterparts which exist in the limit of vanishing μ. The dark solitons travel with constant speed, which is quite different from the Lieb mode, where profiles with different speeds, bounded above by sound velocity can exist for specified interaction strengths. A loss term in the Gross-Pitaevskii equation is dealt with in an external trap along the axial direction and found not to alter the soliton's character.

3.1 Introduction

The dynamics of non-linear waves in Bose-Einstein condensate (BEC) is a subject of immense theoretical and experimental interest in current literature. The recent observation of dark [1], bright solitons [2, 3, 4, 5], soliton trains [6] and Faraday waves [7] have given considerable impetuous to the investigation of the

formation mechanism and control of various non-linear excitations in the quasi-1D scenario [8]. The mean field equation, governing the dynamics of BEC, is the non-linear Schrödinger equation with a harmonic trap. The non-linearity, originating from the two-body interaction, is characterized by the s-wave scattering length 'a', which can be controlled through Feshbach resonance [9], as also the width of the transverse profile [7]. For $a > 0$, elastic interaction is repulsive and the BEC is stable. Negative scattering length implies attractive interaction, where the condensate is found to be stable up-to a certain limit of the number of atoms [10, 11, 12].

The three-body interaction can be generally treated as a perturbation over the two-body case; it becomes significant for short range and larger scattering length [13, 14, 15]. Theoretical and experimental studies [13, 14, 15, 16, 17] for Rb-BEC indicate that, the real part of the three-body interaction term can be $10^3 - 10^4$ times larger than the imaginary part. We confine ourselves in this regime, away from the Feshbach resonance, and do not consider the three-body recombination here, when the corresponding coupling constant is imaginary. A number of theoretical studies have been carried out considering three body interaction in both three- and quasi-one-dimensions [18, 19, 20, 21, 22, 23]. Localized *sech* and power-law type solutions have been obtained [24, 25, 26]. Dark soliton of secant hyperbolic form manifested in purely repulsive three-body interaction regime [25], relevant for Tonks-Girardeau gas [27, 28, 29]. In this case, the soliton velocity is bounded above by sound velocity. Real solitons of both types were also analyzed in [26], where the algebraic one was found to exist only in the $\mu \to 0$ limit and was unstable. The instability of a real soliton envelope has been studied rigorously by Pelinovsky *et al.* [30], and Micallef *et al.* [31]. They have observed generation of a self similar sech-type solution from the collapse of the algebraic one.

In this chapter, we demonstrate the existence of power-law type complex solitons in the presence of repulsive two- and attractive three-body interactions. Unlike the real case, the obtained dark and bright soliton solutions can exist for non-vanishing μ and are stable. The dark solitons have a constant velocity determined by the interaction strengths, which is quite different from the Lieb mode case [25]. Their profiles can change as a function of the param-

eters of the theory. The corresponding velocities change from zero to sound velocity. Interestingly, in the parameter domain where soliton velocity equals sound velocity, it is found that the Bogoliubov dispersion is of quadratic type. For specificity, we consider ^{87}Rb with $m = 1.44 \times 10^{-25}$ Kg and the axial density σ_0 in the range $5.43 \times 10^{7}\text{cm}^{-1} - 9.67 \times 10^{8}\text{cm}^{-1}$. The transverse trap-frequency is taken as $\omega_\perp = 2\pi \times 140$ rad/sec and the two-body coupling constant $g_2 = 4.95\hbar \times 10^{-11}\text{cm}^3/\text{sec}$. The three-body interaction coefficient g_3 has already been estimated [15, 32, 33, 34, 35]. The above parameters allow the present solitons to exist, in the domain of g_3, taking values from $-10^{-27}\text{cm}^6/\text{sec}$ to $-10^{-26}\text{cm}^6/\text{sec}$ (scaled by $\hbar$). This is in the range of theoretically predicted value for ^{87}Rb. In the presence of a trap, the loss term does not significantly alter the profile of the soliton. A linear stability analysis using spectral method is carried out, which shows that the obtained solutions are stable against small perturbations in both dark and bright soliton regimes. Modulational instability (MI) analysis [36, 37, 38] reveals that the parameter regimes relevant for the solutions are away from the domain of instability.

3.2 Power-law complex soliton

The 3D Gross-Pitaevskii (GP) equation for the wave function $\Psi(r,t)$, with an additional three-body interaction, is given by

$$i\hbar\frac{\partial\Psi}{\partial t} = -\frac{\hbar^2}{2m}\nabla^2\Psi + \left(V + g_2|\Psi|^2 + g_3|\Psi|^4 - \mu\right)\Psi, \tag{3.1}$$

where μ is the chemical potential. The cylindrical harmonic trap is given by $V = m\omega_\perp^2(x^2+y^2)/2$ with a tight transverse confinement. For sufficiently small transverse dimension of the cloud, the wave function can be written as $\psi(r,t) = f(z,t)\,\phi_0$ with $\phi_0 = \sqrt{\frac{1}{\pi a_\perp^2}}\exp(-\frac{x^2+y^2}{2a_\perp^2})$ and $a_\perp = \sqrt{\hbar/(m\omega_\perp)}$. The longitudinal envelope function $f(z,t)$ obeys [39, 40],

$$i\hbar\frac{\partial f}{\partial t} = -\frac{\hbar^2}{2m}\frac{\partial^2 f}{\partial z^2} + \left(\tilde{g_2}|f|^2 + \tilde{g_3}|f|^4 - \mu\right)f, \tag{3.2}$$

where the reduced interaction coefficients are

$$\tilde{g_2} = \frac{m\omega_\perp}{2\pi\hbar}\,g_2, \quad \tilde{g_3} = \frac{m^2\omega_\perp^2}{3\pi^2\hbar^2}\,g_3. \tag{3.3}$$

For the space-time independent solution, chemical potential can be written in terms of the asymptotic density σ_0;

$$\mu = (\tilde{g}_2 + \tilde{g}_3\sigma_0)\sigma_0. \tag{3.4}$$

The superfluid velocity is obtained from the continuity equation:

$$v = u(1 - \frac{\sigma_0}{\sigma}), \tag{3.5}$$

where $v = \frac{\hbar}{m}\frac{\partial\theta}{\partial\xi}$ and $f = \sqrt{\sigma(\xi)}\,e^{i\theta(\xi)}$. The hydrodynamic equation for the density is then,

$$\begin{aligned} -\frac{\hbar^2}{2m}(\sigma_z^2 - 2\sigma\sigma_{zz}) &= 4\tilde{g}_3\sigma^4 + 4\tilde{g}_2\sigma^3 \\ &- (4\mu + 2mu^2)\sigma^2 + 2mu^2\sigma_0^2. \end{aligned} \tag{3.6}$$

A power law ansatz

$$\sigma(\xi) = \sigma_0\left(1 - \frac{B}{1 + D\xi^2}\right), \tag{3.7}$$

is found to solve Eq. 3.6, where B and D are given by,

$$\begin{aligned} B = \frac{3\tilde{g}_2 + 8\tilde{g}_3\sigma_0}{2\tilde{g}_3\sigma_0}, \quad D = -\frac{m}{\hbar^2}\frac{(3\tilde{g}_2 + 8\tilde{g}_3\sigma_0)^2}{6\tilde{g}_3}, \\ \text{with} \quad u = \pm\Big(\frac{\tilde{g}_2\sigma_0 + 2\tilde{g}_3\sigma_0^2}{m}\Big)^{\frac{1}{2}}. \end{aligned} \tag{3.8}$$

It is transparent that, non-singular solutions exist only when $\tilde{g}_3$ is negative, i.e., attractive three-body interaction. The value of $\tilde{g}_2$ should be positive from the reality of the soliton velocity, implying repulsive two-body interaction. As mentioned before, u is a constant for given parameter values and density. This situation is quite different from the Lieb-mode case, where the soliton velocity can take different values, bounded above by the sound velocity. The obtained solutions can be categorized into three different classes depending on the values of $\tilde{g}_3$ for a given $\tilde{g}_2$ and σ_0: (i) A dark solition in the range $-\tilde{g}_2/2\sigma_0 \leq \tilde{g}_3 < -3\tilde{g}_2/8\sigma_0$, (ii) a constant background for $\tilde{g}_3 = -3\tilde{g}_2/8\sigma_0$ and (iii) a bright soliton for $-3\tilde{g}_2/8\sigma_0 \leq \tilde{g}_3 < -0.28\tilde{g}_2/\sigma_0$. In these regimes μ is a real positive quantity. For $\mu = 0$, one only obtains a real soliton [26]. Figure 3.1 shows the density profiles of dark and bright solitions for different values of $\tilde{g}_3$. Usually, repulsive interaction alone creates dark soliton, whereas attractive one results in bright solitons in BEC. As

both types of forces are present in the present system, one gets dark and bright solitons, depending on the values of the coupling constants $\tilde{g}_2$ and $\tilde{g}_3$. In Fig. 3.1, $\tilde{g}_3$ is increased from dark to bright soliton for a particular value of $\tilde{g}_2$. The density profile smoothly transits from dark soliton to the bright one. Hence, larger the value of three-body interaction, greater is the accumulation of atoms in the condensate. Physically it amounts to increasing the local density of atoms for going from dark to bright regime. This leads to a depletion of atoms in the background. The solid line in Fig. 3.1 corresponds to $u = 0$ case. Thick solid line is the homogeneous background $\sigma = \sigma_0$, where $u = \pm\frac{1}{2}\sqrt{g_2\sigma_0/m}$.

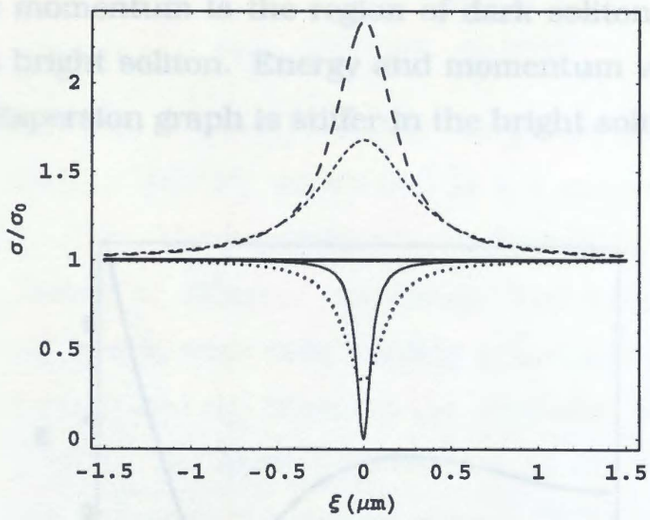

Figure 3.1: The density profiles of soliton solutions for different three-body interactions with $g_2 = 4.95\hbar \times 10^{-11}\text{cm}^3/\text{sec}$. The obtained dark solitions for $\tilde{g}_3 = -\tilde{g}_2/2\sigma_0$ (solid line), $\tilde{g}_3 = -0.45\tilde{g}_2/\sigma_0$ (dotted line) and bright solitons for $\tilde{g}_3 = -0.32\tilde{g}_2/\sigma_0$ (small-dashed line), $\tilde{g}_3 = -0.28\tilde{g}_2/\sigma_0$ (long-dashed line). The thick solid line represents the constant background density σ_0 for $\tilde{g}_3 = -3\tilde{g}_2/8\sigma_0$.

The appropriately normalized energy functional

$$E = \int \Big[\frac{\hbar^2}{2m}\frac{\partial f}{\partial z}\frac{\partial f^*}{\partial z} + \frac{\tilde{g}_2}{2}(ff^*)^2 - \frac{\tilde{g}_2}{2}\sigma_0^2 + \frac{\tilde{g}_3}{3}(ff^*)^3 - \frac{\tilde{g}_3}{3}\sigma_0^3 - \mu(ff^* - \sigma_0)\Big]dz,$$

yields

$$E = \sqrt{\frac{3\pi^2\hbar^2}{2m}}\,\frac{\tilde{g}_2\,|3\tilde{g}_2 + 8\tilde{g}_3\sigma_0|}{16|\tilde{g}_3|^{3/2}}, \tag{3.9}$$

for the soliton profile. Dark soliton with $u = 0$ corresponds to energy $E = \pi\hbar\sigma_0 \times \sqrt{3\tilde{g}_2\sigma_0/(64m)}$, whereas it goes to zero when the background is uniform. Momentum of the condensate profile

$$P = \frac{-i\hbar}{2}\int dz[f^* f_z - f_z^* f] = m\int dz(\sigma - \sigma_0)v(z),$$

gives

$$P = \pi\hbar\sigma_0 \frac{u}{|u|}\left(1 - \sqrt{\frac{3(\tilde{g}_2 + 2\tilde{g}_3\sigma_0)}{-2\tilde{g}_3\sigma_0}}\right). \tag{3.10}$$

It reaches maximum value ($P_{\max} = \pi\hbar\sigma_0$) when $\tilde{g}_3 = -\tilde{g}_2/(2\sigma_0)$. Figure 3.2 depicts the variation of energy with momentum for different three-body interaction strengths. Positive momentum is the region of dark soliton, where as negative one corresponds to bright soliton. Energy and momentum vanish at the transition point $\sigma = \sigma_0$. Dispersion graph is stiffer in the bright soliton regimes.

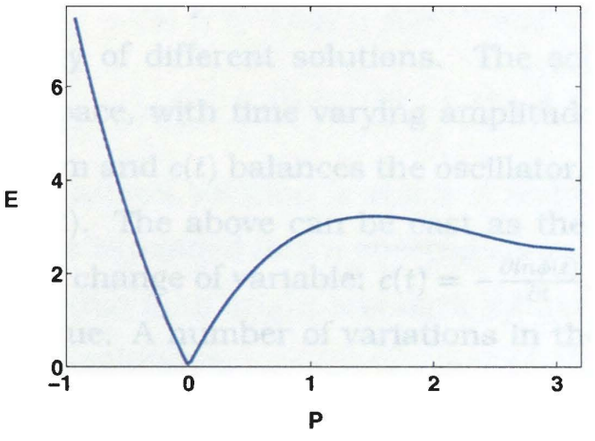

Figure 3.2: Energy vs momentum for the dark and bright solitons for $-\tilde{g}_2/2\sigma_0 \leq \tilde{g}_3 \leq -0.32\tilde{g}_2/\sigma_0$ with the same g_2 used in Fig. 3.1. Energy and momentum are respectively scaled by $\hbar^2{\sigma_0}^2/m \times 10^{-4}$ and $\hbar\sigma_0$.

The number of atoms in the condensate, normalized to vanish at $\sigma = \sigma_0$,

$$N = \left(\frac{3\pi^2\hbar^2\sigma_0^2}{m|\tilde{g}_3|}\right)^{1/2} |3\tilde{g}_2 + 8\tilde{g}_3\sigma_0|, \tag{3.11}$$

shows that the maximum deficiency of atoms in the dark soliton regime is $N = (6\pi\hbar^2\sigma_0^3\tilde{g}_2/m)^{1/2}$.

3.3 Algebraic soliton in a lossy trap

In the following, we analyze the solitons in the presence of harmonic confinement with time dependent nonlinearities and a phenomenological loss term. After suitable scaling, the GP equation is cast in the form [8]

$$i\partial_t\psi = -\frac{1}{2}\partial_{zz}^2\psi + \gamma_2(t)|\psi|^2\psi + \gamma_3(t)|\psi|^4\psi + \frac{1}{2}M(t)z^2\psi + \frac{i\kappa(t)}{2}\psi - \tilde{\mu}(t)\psi. \quad (3.12)$$

$\kappa(t)$ is time dependent loss term. We consider the following ansatz solution for $\psi(z,t)$,

$$\psi(z,t) = B(t)\sqrt{F(T)}e^{\left[i\Phi(z,t)+\frac{1}{2}G(t)\right]}, \quad (3.13)$$

where $T = A(t)\{z - l(t)\}$ and $G(t) = \int_0^t \kappa(t')dt'$. The phase has been taken in the form $\Phi(z,t) = a(t) + b(t)z - \frac{1}{2}c(t)z^2$, where $a(t)$ is a z independent phase term: $a(t) = a_0 - \lambda/2 - \frac{1}{2}\int_0^t A^2(t')dt'$. The parameter λ characterizing the time dependent phase specifies the energy of different solutions. The solutions are necessarily chirped in time and space, with time varying amplitude and width. $b(t)$ is a time dependent momentum and $c(t)$ balances the oscillator, leading to the Riccati equation: $c_t - c^2(t) = M(t)$. The above can be cast as the familiar Schrödinger eigen value equation via a change of variable: $c(t) = -\frac{\partial ln\phi(t)}{\partial t}$. The constant part of $M(t)$ acts as the eigen value. A number of variations in the oscillator frequency can be analytically incorporated from solvable quantum mechanical problems. The oscillator can also be made expulsive. The location of the condensate profile satisfies, $dl(t)/dt + c(t)l(t) = b(t)$. Other parameters are obtained using the following consistency conditions: $B(t) = B_0\ exp(1/2\int_0^t c(t')dt')$ and $A(t) = B^2(t) = b(t)$. The distributed density $F(T)$ satisfies Eq. (3.6) and the solution (7.18) under the following conditions

$$\gamma_2(t) = \frac{m}{\hbar^2}\tilde{g}_2A(t)e^{-G(t)},\ \tilde{\mu}(t) = \frac{m}{\hbar^2}A(t)^2\mu \quad (3.14)$$

$$\gamma_3(t) = \frac{m}{\hbar^2}\tilde{g}_3e^{-2G(t)},\quad and\ \lambda = -\frac{m^2u^2}{\hbar^2}$$

We note that the nonlinearity coefficients and loss are interrelated. $\gamma_2(t)$ has the oscillator dependence through $A(t)$. Soliton profile is not significantly affected by

loss term. It can be compressed and its center of mass can be made to have desired dynamics through parametric manipulation.

3.4 Stability of solitons:

We now analyze the dynamical stability of obtained solutions using the spectral method [41, 42]. A small perturbation $e^{\lambda t}\phi(\xi)$ of soliton solution satisfies $\mathbf{A}\,\vec{\varphi} = \hbar\lambda\,\mathbf{J}\,\vec{\varphi}$, where $\vec{\varphi}$ is a two-dimensional vector and its components are real and imaginary parts of the perturbation: $\vec{\varphi} = (\phi_1\ \phi_2)^T$. Here, J is a two-dimensional matrix with $J_{11} = J_{22} = 0$ and $J_{12} = -J_{21} = 1$. The elements of the matrix operator A are

$$\begin{aligned}
A_{11} &= \frac{\hbar^2}{2m}\frac{\partial^2}{\partial\xi^2} - \tilde{g}_2(3f_1^2 + f_2^2) - \tilde{g}_3(5f_1^4 + f_2^4 + 6f_1^2 f_2^2) + \mu, \\
A_{12} &= \hbar u\frac{\partial}{\partial\xi} - 2\tilde{g}_2 f_1 f_2 - 4\tilde{g}_3 f_1 f_2 |f|^2, \\
A_{21} &= -\hbar u\frac{\partial}{\partial\xi} - 2\tilde{g}_2 f_1 f_2 - 4\tilde{g}_3 f_1 f_2 |f|^2 \quad \text{and} \\
A_{22} &= \frac{\hbar^2}{2m}\frac{\partial^2}{\partial\xi^2} - \tilde{g}_2(f_1^2 + 3f_2^2) - \tilde{g}_3(f_1^4 + 5f_2^4 + 6f_1^2 f_2^2) + \mu,
\end{aligned}$$

where $f = (f_1 + i\,f_2)$. The soliton solution is stable if real part of the eigenvalue λ is negative. ϕ_1 and ϕ_2 are expanded into a spectral series over 800 modes. This numerical analysis shows that both bright and dark solitons solutions are stable in the entire domain of the solutions.

It is now worth investigating the issue of modulation instability since the three-body interaction is attaractive. Phenomenon of modulational instability has been extensively investigated in literature for BEC [43, 44, 45]. A single component BEC with an attractive atom-atom interaction, can result in modulational instability, when the density of atoms exceeds a certain critical value. We assume $f = (f_0 + \tilde{f})exp(i\tilde{\phi})$, where the infinitesimal fluctuation $\tilde{f}$ is given by $\tilde{f} = \tilde{f}_1 cos(Kz - \Omega t) + i\tilde{f}_2 sin(Kz - \Omega t)$. Ω and K are respectively, the frequency and propagation constant, of the modulated wave. The above transformation produces two sets of equations involving $\tilde{f}_1$ and $\tilde{f}_2$. Non trivial solutions are obtained only if K and Ω satisfy the dispersion relation, $2m\Omega^2 = K^2(\hbar^2K^2/2m - 4|\tilde{g}_3|{f_0}^4 + 2\tilde{g}_2{f_0}^2)$,

where $\tilde{g_3} < 0$ and $\tilde{g_2} > 0$. If $\hbar^2 K^2/2m < (4|\tilde{g_3}|{f_0}^4 - 2\tilde{g_2}{f_0}^2)$, it would show modulation instability. This condition immediately implies $\tilde{g_2} < 2|\tilde{g_3}|\sigma_0$, which is not in the allowed parameter range for the obtained solutions. Thus our solutions are modulationally stable.

References

[1] S. Burger *et al.*, Phys. Rev. Lett. **83**, 5198 (1999); J. Denshlag *et al.*, Science **287**, 97 (2000).

[2] U. Al Khawaja, H. T. C. Stoof, R. G. Hulet, K. E. Strecker, and G. B. Partridge, Phys. Rev. Lett. **89**, 200404 (2002).

[3] L. Khaykovich *et al.*, Science **296**, 1290 (2002).

[4] K. E. Strecker *et al.*, New J. Phys. **5**, 73 (2003).

[5] S. L. Cornish, S. T. Thompson, and C. E. Wieman, Phys. Rev. Lett. **96**, 170401 (2006).

[6] K. E. Strecker, G. B. Patridge, A. G. Truscott, and R. G. Hulet, Nature **417**, 150 (2002).

[7] K. Staliunas, S. Longhi, and G. J. de Valcárcel, Phys. Rev. Lett. **89**, 210406 (2002).

[8] R. Atre, P. K. Panigrahi, and G. S. Agarwal, Phys. Rev. E **73**, 056611 (2006) and references therein.

[9] S. Inouye, M. R. Andrews, J. Stenger, H.-J. Miesner, D. M. Stamper-Kurn, and W. Ketterle, Nature (London) **392**, 151 (1998).

[10] F. Dalfovo and S. Stringari, Phys. Rev. A **53**, 2477 (1996).

[11] R. J. Dodd *et al.*, Phys. Rev. A **54**, 661 (1996).

[12] C. C. Bradley, C. A. Sackett, and R. G. Hulet, Phys. Rev. Lett. **78**, 985 (1997).

[13] A. E. Leanhardt *et al.*, Phys. Rev. Lett. **89**, 040401 (2002).

[14] P. Pieri, and G. C. Strinati, Phys. Rev. Lett. **91**, 030401 (2003).

[15] T. Köhler, Phys. Rev. Lett. **89**, 210404 (2002).

[16] B. Laburthe Tolra *et al.*, Phys. Rev. Lett. **92**, 190401 (2004).

[17] J. Söding *et al.*, Appl. Phys. B: Laser Opt. **69**, 257 (1999).

[18] E. B. Kolomeisky, and J. P. Straley, Phys. Rev. B **46**, 11749 (1992).

[19] N. Akhmediev, M. P. Das, and A. V. Vagov, Int. J. Mod. Phys. B **13**, 625 (1999).

[20] E. B. Kolomeisky, T. J. Newman, J. P. Straley, and X. Qi, Phys. Rev. Lett. **85**, 1146 (2000).

[21] V. A. Brazhnyi, V. V. Konotop, and L. P. Pitaevskii, Phys. Rev. A **73**, 053601 (2006).

[22] R. Pardo, and V. M. Pérez-García, Phys. Rev. Lett. **97**, 254101 (2006).

[23] A. -X. Zhang, and J. -K. Xue, Phys. Rev. A **75**, 013624 (2007).

[24] R. K. Bhaduri, S. Ghosh, M. V. N. Murthy, and D. Sen, J. Phys. A **34**, 6553 (2001).

[25] M. Ögren and G. M. Kavoulakis and A. D. Jackson, Phys. Rev. A **72**, 021603(R) (2005).

[26] L. Khaykovich, and B. A. Malomed, Phys. Rev. A **74**, 023607 (2006).

[27] L. Tonks, Phys. Rev. **50**, 955 (1936); M. Girardeau, J. Math. Phys. **1**, 516 (1960).

[28] B. Paredes et al., Nature London **429**, 277 (2004).

[29] T. Kinoshita et al., Science **305**, 1125 (2004).

[30] D. E. Pelinovsky, V. V. Afanasjev, Y. S. Kivshar, Phys. Rev. E **53**, 1940 (1996).

[31] R. W. Micallef, V. V. Afanasjev, Y. S. Kivshar, and J. D. Love, Phys. Rev. E **54**, 2936 (1996).

[32] P. F. Bedaque, E. Braaten, and H.-W. Hammer, Phys. Rev. Lett. **85**, 908 (2000).

[33] E. Braaten and H.-W. Hammer, Phys. Rev. Lett. **87**, 160407 (2001).

[34] E. Braaten, H.-W. Hammer, and T. Mehen, Phys. Rev. Lett. **88**, 040401 (2002).

[35] S. P. Tewari, P. Silotia, A. Saxena, and L. K. Gupta, Phys. Lett. A **359**, 658 (2006).

[36] A. Hasegawa, and W. F. Brinkman, IEEE J. Quantum Electron. 16, 694 (1980).

[37] K. Tai, A. Hasegawa, and A. Tomita, Phys. Rev. Lett. **56**, 135 (1986).

[38] G. P. Agrawal, Phys. Rev. Lett. **59**, 880 (1987).

[39] A. D. Jackson, and G. M. Kavoulakis, Phys. Rev. Lett. **89**, 070403 (2002).

[40] L. Salasnich, A. Parola, and L. Reatto, Phys. Rev. A **65**, 043614 (2002).

[41] Y. Y. Su, and B. Khomami, J. Comput. Phys. **100**, 297 (1992).

[42] I. V. Barashenkov, S. R. Woodford, and E. V. Zemlyanaya, Phys. Rev. Lett. **90**, 054103 (2003).

[43] L. Salasnich, A. Parola, and L. Reatto, Phys. Rev. Lett. **91**, 080405 (2003).

[44] L. D. Carr, and J. Brand, Phys. Rev. Lett. **92**, 040401 (2004).

[45] T. S. Raju, P. K. Panigrahi, and K. Porsezian, Phys. Rev. A **71**, 035601 (2005).

Chapter 4

Vibrations as probe of Bose-Einstein condensates in different phases

We study the Faraday pattern in Bose Einstein condensates in various interaction regimes, where the Bogoliubov modes are excited through the temporal oscillation of the transverse trap frequency. In the process one needs to analyze the solution space of Mathieu equation. The Floquet analysis for the obtained Mathieu equations, governing the sound dynamics, reveals that series of resonances exist in the system. The dominant wave numbers of the second sound clearly differentiate strong and weak coupling regimes.

4.1 Introduction

Long time back Faraday had observed that a transverse vibration in a fluid sets up a longitudinal one, whose wave number is governed by the transverse frequency [1]. Recently, in an experiment involving Bose-Einstein condensates, Faraday pattern has been observed in a cigar-shaped BEC involving Bogoliubov modes [2]. As is evident, these excitations reveal the structure of non-linearity in the Gross-Pitaevskii equation, governing the mean field dynamics of BEC.

4.2 Faraday waves in weakly coupled BEC

For quasi-1D, the field equation is given by

$$i\frac{\partial}{\partial t}\psi = \left[-\frac{\partial^2}{\partial z^2} + V(z) + c(t)|\psi|^2\right]\psi, \tag{4.1}$$

where $c(t)$ is the time dependent nonlinearity coefficient. In the flat potential limit (V(z)=0), space-independent solution is of the type,

$$\psi_H = e^{-i\int_0^t c(t')dt'}. \tag{4.2}$$

A spatial perturbative modulation around this seed solution is considered:

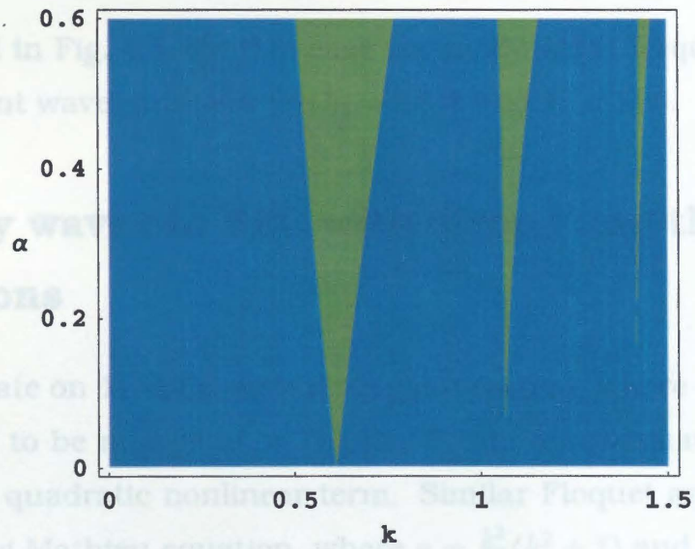

Figure 4.1: Resonance tongues of the GP equation for $\omega = 0.942$.

$$\psi = \psi_H\left[1 + W(t)cos\ kz\right]. \tag{4.3}$$

Here, $W(t)$ is complex valued amplitude of the perturbation: $W(t) = u(t) + iv(t)$. For a periodic temporal modulation of $c(t) = 1 + 2\alpha\ cos\ 2\omega t$, $u(t)$ satisfies

$$\frac{\partial^2 u}{\partial t^2} + \left[k^2(k^2+2) + 4\alpha k^2 cos\ 2\omega t\right]u = 0, \tag{4.4}$$

which is the Mathieu equation:

$$\frac{\partial^2 u}{\partial t^2} + \left[a - 2q\ cos\ \Omega t\right]u = 0, \tag{4.5}$$

with $a = \frac{k^2}{\omega^2}(k^2+2)$ and $q = -2\alpha k^2/\omega^2$. When, $q = 0$ the Mathieu functions are simply $cos(\sqrt{a}t)$ and $sin(\sqrt{a}t)$. For non-zero q, Mathieu functions are only periodic in t for certain values of a, called Mathieu characteristic values. According to Floquet's theorem, any Mathieu function can be written in the form $e^{irt} \times function$, where r is the Floquet characteristic exponent. When r is real, the function is periodic. Floquet analysis of Eq. 4.4 reveals that a series of resonances exist in the system, where the neutral stability curve can be obtained by equating the real part of the characteristic exponent to zero. The dominant wave number in the longitudinal direction satisfies

$$k_n = \left(-1 + \sqrt{1+(n\omega)^2}\right)^{1/2}, \tag{4.6}$$

which is depicted in Fig. 4.1. In this case the modulation frequency $\omega = 0.3 \times \pi$. First two dominant wave numbers are $k_1 = 0.612$ and $k_2 = 1.06$.

4.3 Faraday waves in BEC with strong and three-body interactions

Now we concentrate on 1D-BEC with strong interaction, where the kinetic energy term is assumed to be negligible in Thomas-Fermi approximation [3]. This 1D-GP equation has quadratic nonlinear term. Similar Floquet analysis is done for the corresponding Mathieu equation, where $a = \frac{k^2}{\omega^2}(k^2+1)$ and $q = -\alpha k^2/\omega^2$. The dominant wave numbers are seen to be shifted towards lower values.

$$k_n = \frac{1}{2}\left(-1 + \sqrt{1+4(n\omega)^2}\right)^{1/2}. \tag{4.7}$$

First two resonances occur at $k_1 = 0.75$ and $k_2 = 1.2$. Three-body interaction in BEC becomes significant for high density and large scattering length. In this case, quintic non-linearities will be present in the 1D-GP equation [4]. First two dominant wave numbers are obtained as, $k_1 = 1.373$ and $k_2 = 1.94$, which are shifted towards higher values. Hence, the above analysis reveals that higher nonlinearity produces larger value of the wave numbers. We observe that the interactions remain repulsive for $\alpha < 0.5$. For higher α value, scattering length will change the sign from repulsive to attractive one. As a result resonance tongues

appeared in $k-\alpha$ plot will split into two parts, showing bifurcation nature. We have delineated the difference between this patterns in the weak, strong and three-body coupling scenarios. This pattern can be used as probe of Bose-Einstein condensates in different phases.

References

[1] M. Faraday, Philos. Trans. R. Soc. London **121**, 299 (1831).

[2] P. Engels, C. Atherton and M. A. Hoefer, Phys. Rev. Lett. **98**, 95301 (2007).

[3] Utpal Roy and P. K. Panigrahi, *cond-mat/0703092* (2007).

[4] Utpal Roy, R. Atre, C. Sudheesh, C. N. Kumar, and P. K. Panigrahi, *arXiv:0708.3646* (2007).

Chapter 5

Sinusoidal Excitations in Two Component Bose-Einstein Condensates

The non-linear coupled Gross-Pitaevskii equation governing the dynamics of the two component Bose-Einstein condensate (TBEC) is shown to admit pure sinusoidal, propagating wave solutions in quasi one dimensional geometry. These solutions, which exist for a wide parameter range, are then investigated in the presence of a harmonic oscillator trap with time dependent scattering length. This illustrates the procedure for coherent control of these modes through temporal modulation of the parameters, like scattering length and oscillator frequency. We subsequently analyzed this system in an optical lattice, where the occurrence of an irreversible phase transition from superfluid to insulator phase is seen.

5.1 Introduction

Much theoretical work has already gone into studying the ground state solutions of the coupled Gross-Pitaevskii (GP) equations describing multi-component BECs [1, 2, 3, 4]. TBEC has been observed, where the two hyperfine levels of ^{87}Rb [5, 6] act as the two components. In this case, a fortuitous coincidence in the triplet and singlet scattering lengths has led to the suppression of exoergic spin-exchange collisions, which lead to heating and resultant loss of atoms. A number of interesting features, like the preservations of the total density profile and coherence for a characteristically long time, in the face of the phase-diffusing

couplings to the environment and the complex relative motions [7], point to the extremely interesting dynamics of the TBEC. TBEC has been produced in a system comprising of ^{41}K and ^{87}Rb, in which sympathetic cooling of Rb atoms was used to condense the K atoms [8]. It has also been observed in $^{7}Li-^{133}Cs$ [9] and $^{87}Rb-^{133}Cs$ systems [10].

The presence of nonlinearities in BECs [11], make them ideal candidates for observation of solitary waves, ubiquitous to non-linear media. Delicate balance of dispersion and nonlinearities leads to these waves in a variety of nonlinear physical systems, ranging from hydrodynamics, optical fibers, atomic resonant media to condensed matter and particle physics [12, 13, 14, 15]. Dark solitons in repulsive single component BEC [16, 17] and bright soliton in attractive case [18, 19, 20, 21], have been recently observed, leading to the possibility of realizing coherent atom laser and other applications [22]. In the TBEC, a number of investigations, primarily devoted to the study of localized solitons, have been carried out recently [23, 24, 25, 26, 27]. The coincidence of singlet-triplet coupling in ^{87}Rb, leads to the well known Manakov system [28] in weak coupling quasi-one dimensional scenario [29, 30]. The rich dynamics of solitons in this integrable system has received considerable attention in the literature [31, 32, 33, 34]. The effect of spatial inhomogeneity, three-dimensional geometry, and dissipation on TBEC have been examined. Akin to their optical counterparts, the possibility of exciting dark-bright solitons in repulsively interacting TBEC in ^{23}Na and ^{87}Rb have been pointed out [35]. Dark solitons in TBEC for a miscible case have also been analyzed recently [36]. However, the periodic solitary waves have not received much attention in the literature. Periodic sinusoidal excitations are natural in linear systems. In nonlinear models periodic cnoidal waves can be present. It is worth mentioning that, in non-linear resonant atomic media, cnoidal excitations have been experimentally generated [37, 38], where relaxation naturally led to the atomic level population necessary for the existence of these nonlinear periodic waves [39].

We analyze here solutions of a generic TBEC model in a quasi-one dimensional geometry for periodic solutions. Very interestingly, we find exact sinusoidal wave solutions in this system, which do not occur in the single component case, be-

cause of the non-linearity. The presence of two components leads to these waves, whose energy difference are controlled by the cross phase modulation (XPM). In presence of harmonic oscillator trap, with a time dependent scattering length, these waves can be compressed and accelerated. This leads to the possibility of their coherent control. We then consider our system in an optical lattice [40]. Since an external sinusoidal potential is present here, it would be interesting to see how the periodic sinusoidal excitations are affected by the external potential. We have observed a superfluid to insulator phase transition in this system.

The chapter is organized as follows. In the following section, we study the dynamics of the propagating sinusoidal waves and identify the allowed parameters regimes. In section 5.3, we have investigated the dynamics of these waves with time varying scattering length in a trap. The goal of this study is to illustrate the procedure of coherent control of these modes. The behavior of the stationary sinusoidal excitations in presence of an optical lattice is the subject of study in section 5.4. Phase transition from superfluid to insulator phase, a classical transition known in the literature as dynamical superfluid-insulator phase transition (DSIT) [41, 42, 43], is found to occur here.

5.2 Sinusoidal Solutions of coupled GP equations

In the case of two species condensate with a wave function $\psi_i(x,t)$ for the species i, the coupled quasi-1D GP equation in the presence of an external potential V_i, can be written as,

$$i\hbar\dot{\psi}_1 = -\frac{\hbar^2}{2m}\psi_1'' + V_1(x)\psi_1 + [g_1|\psi_1|^2 + g_{12}|\psi_2|^2 - \nu_1]\psi_1 \quad (5.1a)$$

$$\text{and } i\hbar\dot{\psi}_2 = -\frac{\hbar^2}{2m}\psi_2'' + V_2(x)\psi_2 + [g_{21}|\psi_1|^2 + g_2|\psi_2|^2 - \nu_2]\psi_2. \quad (5.1b)$$

The strength of the intra-species interactions is g_i and ν_j is the chemical potential. We assume the interspecies interaction to be same for both the components: $g_{12} = g_{21}$.

First, we consider two-quasi-1D condensate in absence of a trap, where the traveling wave type ansatz solutions can be written as,

$$\psi_j(x,t) = \sqrt{\sigma_j(x-ut)}e^{i\chi_j(x-ut)}, \quad (5.2)$$

with χ_j being non-trivial phase. It is necessary to assume that both the waves propagate with the same velocity. Current conservation yields,

$$v_j = u(1 - \frac{\sigma_{0j}}{\sigma_j}), \tag{5.3}$$

where $v_j = \frac{\hbar}{m}\chi_j'$. σ_{0j}'s are the equilibrium density of the atoms in this condensed phase. We impose the boundary condition that, as σ_j's approach σ_{0j}'s, the non-trivial phases χ_j's tend to zero. As can be checked by substitutions, Eq. (5.1a) and (5.1b) have the following sinusoidal-wave solutions:

$$\psi_1(x,t) = \sqrt{\sigma_{01}[1 - (1 - \frac{m^2u^2}{\hbar^2})\sin^2(x-ut)]}e^{i[\chi_1(x,t)]}, \tag{5.4a}$$

$$\text{and} \quad \psi_2(x,t) = \sqrt{\sigma_{02}[1 - (1 - \frac{m^2u^2}{\hbar^2})\cos^2(x-ut)]}e^{i[\chi_2(x,t)]}. \tag{5.4b}$$

The phase is given by

$$\chi_1 = \frac{mu}{\hbar}(x - ut) - \tan^{-1}[\frac{mu}{\hbar}\tan(x - ut)], \tag{5.5}$$

with the second component in the same form as the first one, except for having an inverse *cotangent* function instead of the *tangent* one. Although we have taken two phases with different character, solutions where both of them have similar nature can also occur.

The superfluid velocity leads to a periodic current density, having the form,

$$j_1 = \frac{\hbar}{2m}u\sigma_{01}\sin^2(x-ut)$$

$$\text{and} \quad j_2 = \frac{\hbar}{2m}u\sigma_{02}\cos^2(x-ut).$$

For these solutions to exist, it is found that the interactions need to satisfy $g_{12}^2 = g_1g_2$. The background densities are related by $g_1\sigma_{01} = g_{12}\sigma_{02}$. One can see that the intra and the interspecies interactions need to be related for these solutions to exist. The difference between cross phase modulation and self phase modulation is found to sustain these waves, when both the condensates have different chemical potentials: $\nu_1 - \nu_2 = (g_1 - g_{12})\sigma_{01}(1 + \frac{m^2u^2}{\hbar^2}) = (g_{12} - g_2)\sigma_{02}(1 + \frac{m^2u^2}{\hbar^2})$.

5.3 Solutions in presence of Harmonic oscillator trap

The effect of the longitudinal trap on the condensate and soliton profile has been recently investigated quite intensively. In the general scenario, the scattering

length, oscillator frequencies can be time dependent, in addition to the presence of a phenomenological loss term [44, 45, 46, 47]. Below we employ this method to the sinusoidal waves in the two component scenario. As will be seen later, this can be used for controlling the excitations. They may be compressed or accelerated, through suitable temporal modulations of various parameters. We consider self-similar solutions in the oscillator trap $V_j = \frac{1}{2}M(t)x^2$, for which the ansatz solution is of the following form,

$$\psi_j(x,t) = \sqrt{A(t)\sigma_j[A(t)(x-l(t))]}e^{i[\chi_j(x,t)+\phi(x,t)]}. \tag{5.6}$$

Here, $\phi(x,t)$ is a density independent phase having the form $\phi(x,t) = a(t) + b(t)x - \frac{1}{2}c(t)x^2$ and $l(t) = \int_0^t v(t')dt'$. The sinusoidal wave, in this case, is a propagating wave with the velocity $v(t)$ in the moving condensate. We found

$$a(t) = a_0 - \frac{\frac{\hbar^2}{2m} - \bar{\mu}}{\hbar}\int_0^t A^2(t')dt'$$

where $\bar{\mu} = \mu_j + \lambda_j$. Here $\nu_j(t) = \mu_j A^2(t)$ $(j = 1, 2)$ and λ_j's are constant parameters controlling the energy of the excitations. The time dependent wave vector $b(t) = A(t)$ and $c(t)$ can be determined by the Ricatti type equation

$$\hbar\dot{c}(t) - \frac{\hbar^2}{m}c^2(t) = M(t).$$

By choosing $c(t) = -\frac{m}{\hbar}[\frac{\partial}{\partial t}\log\phi(t)]$, this equations can be transformed into the Schrödinger equation $\ddot{\phi} + \frac{M(t)}{m}\phi = 0$. From current conservation, amounting to solving the imaginary part of the coupled GP equations, one gets Eq. (5.3), with the consistency conditions:

$$\begin{aligned} l_t(t) + \frac{\hbar}{m}c(t)l(t) - \frac{\hbar}{m}A(t) &= A(t)u, \quad B(t) = \sqrt{A(t)}, \\ \dot{A}(t) = \frac{\hbar}{m}A(t)c(t) \quad \text{or} \quad & A(t) = \frac{\hbar A_0}{m}\exp\int_0^t c(t')dt', \\ g_j(t) = \kappa_j A(t) \quad \text{and} \quad & g_{12}(t) = \kappa_{12}A(t). \end{aligned}$$

The real part of the coupled GP equations reduces to,

$$\begin{aligned} \frac{\hbar^2}{4m}\sigma_1\sigma_1'' - \frac{\hbar^2}{8m}\sigma_1' + (\frac{1}{2}mu^2 + \lambda_1)\sigma_1^2 - \kappa_1\sigma_1^3 - \kappa_{12}\sigma_2\sigma_1^2 - \frac{1}{2}mu^2\sigma_{01}^2 &= 0 \\ \text{and} \quad \frac{\hbar^2}{4m}\sigma_2\sigma_2'' - \frac{\hbar^2}{8m}\sigma_2' + (\frac{1}{2}mu^2 + \lambda_2)\sigma_2^2 - \kappa_2\sigma_2^3 - \kappa_{12}\sigma_1\sigma_2^2 - \frac{1}{2}mu^2\sigma_{02}^2 &= 0. \end{aligned}$$

Consistency condition requires $\mu = \bar{\mu} = \mu_1 + \lambda_1 = \mu_2 + \lambda_2$. The form of the densities have been found to retain their earlier forms:

$$\psi_1(x,t) = \sqrt{A(t)\sigma_{01}[1-(1-\frac{m^2u^2}{\hbar^2})\sin^2[A(t)(x-l(t))]]}e^{i[\chi_1(x,t)+\phi(x,t)]}$$

$$\text{and } \psi_2(x,t) = \sqrt{A(t)\sigma_{02}[1-(1-\frac{m^2u^2}{\hbar^2})\cos^2[A(t)(x-l(t))]]}e^{i[\chi_2(x,t)+\phi(x,t)]}.$$

The non-trivial phases are now controlled by the trap:

$$\chi_1 = \frac{mu}{\hbar}A(t)[x-l(t)] - \tan^{-1}[\frac{mu}{\hbar}\tan[A(t)(x-l(t))]],$$

with a corresponding expression for the second component. The superfluid current densities in presence of the trap takes the form

$$j_1' = \frac{\hbar\sigma_{01}}{2m}((u+A(t)-c(t)x)(\frac{m^2u^2}{\hbar^2}-1)\sin^2[A(t)(x-l(t))])$$

with a similar expression for the second component.

Unlike the previous case, where the flow density is periodic, here it gets modulated by the chirped phase. Explicitly, it depends on the oscillator potential. Hence, by tuning the trap the current densities can be controlled suitably.

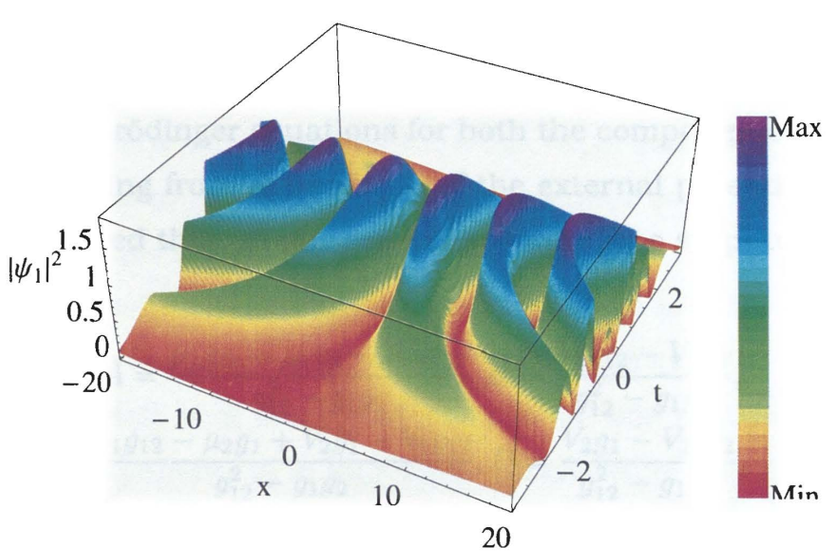

Figure 5.1: Density distribution of the sinusoidal wave of the first component for ^{87}Rb in presence of a regular oscillator trap with $\kappa_1 = 0.4$ and $\kappa_2 = 0.1$.

Some constraint relations, which restrict our solutions, have to be satisfied. The difference between the chemical potentials, $\lambda_1 - \lambda_2 = (\kappa_1 - \kappa_{12})\sigma_{01}(1+\frac{m^2u^2}{\hbar^2}) = (\kappa_{12}-\kappa_2)\sigma_{02}(1+\frac{m^2u^2}{\hbar^2})$ with the constraint $\kappa_{12}^2 = \kappa_1\kappa_2$ and $\kappa_1\sigma_{01} = \kappa_{12}\sigma_{02}$.

For illustration, we consider the regular oscillator with $M(t) = \alpha^2$, and inter-species interactions $\kappa_1 = 0.4$ and $\kappa_2 = 0.1$. The equality of the SPM and XPM leads to the same background along with the same chemical potentials for the both the component. Fig.(5.1) shows the traveling wave, with a time dependent velocity in the presence of the trap. In presence of oscillator, the atoms can be accelerated and suitably controlled.

5.4 Solutions in presence of an Optical lattice

We now consider situation where the two species are loaded in an optical lattice, where the potentials experienced by the two components can have different depth: $V_j = V_j \cos^2 x$ (j=1,2). The solutions are taken to be of the form,

$$\psi_1(x,t) = \sqrt{A + B\cos^2(x)}e^{i\chi_1(x)+i\omega_1 t} \text{ and} \tag{5.8}$$

$$\psi_2(x,t) = \sqrt{C + D\cos^2(x)}e^{i\chi_2(x)+i\omega_2 t}, \tag{5.9}$$

with $\omega_j = \frac{1}{2} + \bar{\mu_j}$ and $\chi_{jz} = \frac{2c_j}{\rho_j^2}$ $(j = 1, 2)$. Here, $c_j's$ are the integration constants. Earlier these type of solutions have been considered for TBEC in a trap [48]. In these so called balanced solutions, the sinusoidal solutions simultaneously satisfy the linear Schrödinger equations for both the components, as well as algebraic equations coming from the balance of the external potential with the non-linearity. It is observed that, in our general scenario, the amplitude relations are unaltered:

$$A = \frac{\mu_2 g_{12} - \mu_1 g_2 - 2V_2 g_{12}}{g_{12}^2 - g_1 g_2}, B = \frac{V_2 g_{12} - V_1 g_2}{g_{12}^2 - g_1 g_2}, \tag{5.10}$$

$$C = \frac{\mu_1 g_{12} - \mu_2 g_1 + V_2 g_1 - V_1 g_{12}}{g_{12}^2 - g_1 g_2}, D = \frac{V_2 g_1 - V_1 g_{12}}{g_{12}^2 - g_1 g_2}, \tag{5.11}$$

with $\mu_j = \nu_j + \bar{\mu_j}$. Dispersion only affects the super-current through the integration constants: $I_1 = \frac{1}{2}AB + (\frac{1}{2} + \mu_1)A^2 - g_2 A^3 - g_{12}(C + D)A^2 + V_1 A^2$, where, $I_j = \frac{\hbar^2 c_j^2}{2m}$. For the second component, integration constant will have the same form with the corresponding amplitude, background and chemical potential. The first term in this expression corresponds to the dispersion. The non-trivial phase for the first component has the explicit form: $\chi_1(z) = c_1 \tan^{-1}[\frac{\sqrt{A+B}\tan(z)}{\sqrt{A}}]/\sqrt{A(A+B)}$. Similar type of expression holds true for the second component. One can calculate the

superfluid velocity $v_j's$, which leads to a constant flow density $J_j's$ for the superfluid phase, as in the single component case. By tuning the trap frequency, we can control the superfluid velocity. Interplay between non-linearity and potential strength guarantees periodic form of the solution. The components can occupy the peaks or the valleys depending upon the experimental parameter values. If A, B, C, D are all positive, then first component will occupy the peaks, while the second component will move to the valleys of the optical potential. The most stable configuration is the one, in which, both species occupy the valleys of the lattice potential for which $B < 0$ and $|A| > |B|$.

The total energy of the system, when both the species have non-zero current density is,

$$\begin{aligned} E_{SF} &= \frac{\pi}{2}[2(A+C)+B+D]+2\pi(\sqrt{A(A+B)}+\sqrt{C(C+D)})+\frac{\pi}{8}[(8A^2+8AB+3B^2)g_1 \\ &+(8C^2+8CD+3D^2)g_2+g_{12}(4A(2C+D)+(B(4C+D)))]+\frac{\pi}{4}[V_1(4A+3B) \\ &+V_2(4C+D)]-\pi[\mu_1(2A+B)+\mu_2(2C+D)]-2\pi\left(\frac{c_1^2}{\sqrt{A(A+B)}}+\frac{c_2^2}{\sqrt{C(C+D)}}\right). \end{aligned}$$

It carries the signature of the transition of respective species from superfluid to insulating regime. It is worth observing that, the superfluid energy is different for this case as compared to the earlier obtained balanced solutions. The difference precisely arises through the integration constants.

At the transition point, the atomic quasi-clusters get localized, indicating zero current density. The corresponding energy is analytic everywhere. Either both the components transit in a correlated manner or one can have situations in which one of the components is in superfluid phase while the other is in insulating phase. Accordingly, we can have superfluid-superfluid, superfluid-insulator, insulator-superfluid and insulator-insulator mixtures. For example, considering non-zero backgrounds, above energy function becomes non-analytic at points,

$$\begin{aligned} V_{1c} &= \frac{1}{2}\mu_1-\frac{g_1(3\mu_1 g_2-\mu_2 g_{12})}{2(g_{12}^2+g_1 g_2)}, \\ V_{2c} &= \mu_2-\frac{g_2(3\mu_2 g_1+3\mu_1 g_{12})}{2(g_{12}^2+g_1 g_2)}, \end{aligned}$$

at which the two component condensate is in the insulating phase. The corresponding insulating wave functions are,

$$\begin{aligned} \psi_1'(z,t) &= 0.5\sqrt{A}e^{iz}(1-e^{-2iz})e^{i(\frac{1}{2}+\bar{\mu_1})}, \\ \psi_2'(z,t) &= 0.5\sqrt{C}e^{iz}(1+e^{-2iz})e^{i(\frac{1}{2}+\bar{\mu_1})}, \end{aligned} \tag{5.12}$$

where, $A = (\mu_2 g_{12} + \mu_1 g_2)(g_{12}^2 + 2g_1 g_2)/(g_1^2 g_2^2 - g_{12}^4)$ and $C = (\mu_1 g_{12} - \mu_2 g_1)/(g_{12}^2 - g_1 g_2)$. The energy of the superfluid phase is found to be less compared to that of insulator phase. As is evident, the interactions play a crucial role in the transition.

References

[1] T. L. Ho, and V. B. Shenoy, Phys. Rev. Lett. **77**, 3276 (1996).

[2] H. Pu, and N. P. Bigelow, Phys. Rev. Lett. **80**, 1130 (1998).

[3] Q.Han Park, and J. H. Eberly, Phys. Rev. Lett. **85**, 4195 (2000).

[4] Q.Han Park, and J. H. Eberly, Phys. Rev. A **70**, 021602(R) (2004).

[5] C. J. Myatt, E.A. Burt, R. W. Ghrist, E.A. Cornell, and C. E. Wieman, Phys. Rev. Lett. **78**, 586 (1997).

[6] D. S. Hall, M.R. Matthews, J. R. Ensher, C. E. Wieman and E. A. Cornell, Phys. Rev. Lett. **81**, 1539 (1998).

[7] M. R. Matthews *et al.*, Phys. Rev. Lett. **83**, 3358 (1999).

[8] G. Modugno, G. Ferrari, G. Roati, R. J. Brecha, A. Simoni, and M. Inguscio, Science **294**, 1320 (2001).

[9] M. Mudrich, S. Kraft, K. Singer, R. Grimm, A. Mosk, and M. Weidemüller, Phys. Rev. Lett. **88**, 253001 (2002).

[10] M. Haas *et al.*, New J. Phys. **9**, 147 (2007).

[11] C. J. Pethik, and H. Smith, *Bose-Einstein Condensation in Dilute Gases* (Cambridge University Press, Cambridge, 2002).

[12] L. Allen and J.H. Eberly, *Optical Resonances and Two-Level Atoms* (Dover, New York, 1987) and references therein.

[13] A. Das, *Integrable Models* (World Scientific, Singapore, 1989).

[14] M. Remoissenet, *Waves Called Solitons: Concepts and Experiments* (Springer-Verlag, Heidelberg, 1999).

[15] G. P. Agrawal, *Nonlinear Fiber Optics* (Academic Press, Boston, 2007).

[16] S. Burger *et al.*, Phys. Rev. Lett. **83**, 5198 (1999).

[17] J. Denshlag *et al.*, Science **287**, 97 (2000).

[18] K. E. Strecker *et al.*, Nature (London) **417**, 150 (2002).

[19] U. Al Khawaja, H. T. C. Stoof, R. G. Hulet, K. E. Strecker, and G.B. Partridge, Phys. Rev. Lett. **89**, 200404 (2002).

[20] L. Khaykovich *et al.*, Science **296**, 1290 (2002).

[21] K. E. Strecker, G. B. Partridge, A. G. Truscott and R.G. Hulet, New Journal of Phys. **5**, 73 (2003).

[22] W. Ketterle, Rev. Mod. Phys. **78**, 483 (2006).

[23] B. P. Anderson *et al.*, Phys. Rev. Lett. **86**, 2926 (2001).

[24] R. Nath, P. Pedri, and L. Santos, *cond-mat/0610703* (2006).

[25] M. Matuszewski, B. A. Malomed, and M. Trippenbach, Phys. Rev. A **76**, 043826 (2007).

[26] T. Kanna, M. Vijayajayanthi, and M. Lakshmanan, Phys. Rev. A **76**, 013808 (2007).

[27] A. Gubeskys, and B. A. Malomed, *arXiv:0708.4028* (2007); A. Gubeskys, and B. A. Malomed, *arXiv:0705.0364* (2007).

[28] S.V. Manakov, Sov. Phys. JETP **38**, 248 (1974).

[29] A. D. Jackson, and G. M. Kavoulakis, Phys. Rev. Lett. **89**, 070403 (2002).

[30] L. Salasnich, A. Parola, and L. Reatto, Phys. Rev. A **65**, 043614 (2002).

[31] T. Kanna, and M. Lakshmanan, Phys. Rev. Lett. **86**, 5043 (2001).

[32] T. Kanna, and M. Lakshmanan, Phys. Rev. E **67**, 46617 (2003).

[33] N. Lazarides, and G. P. Tsironis, Phys. Rev. E **71**, 036614 (2005).

[34] S. A. Derevyanko, J.E. Prilepsky, and D.A. Yakushev, J. Phys. A: Math. Gen. **39**, 1297 (2006).

[35] Th. Busch and J.R. Anglin, Phys. Rev. Lett. **87**, 010401 (2001).

[36] P. Öhberg and L. Santos, Phys. Rev. Lett. **86**, 2918 (2001).

[37] M. A. Newbold and G.J. Salamo, Phys. Rev. Lett. **42**, 887 (1979).

[38] J. L. Shultz and G.J. Salamo, Phys. Rev. Lett. **78**, 855 (1997).

[39] P. K. Panigrahi and G.S. Agarwal, Phys. Rev. A **67**, 033817 (2003).

[40] I. Bloch, J. Dalibard, and W. Zwerger, *arXiv: 0704.3011* (2007) and references therein.

[41] A. Smerzi, A. Trombettoni, P. G. Kevrekidis, and A.R. Bishop, Phys. Rev. Lett. **89**, 170402 (2002).

[42] M. Vyas, P. Das, and P. K. Panigrahi, *arXiv:0712.0880* (2007).

[43] E. Altman, Y. Kafri, A. Polkovnikov, and G. Refael, *arXiv:0711.2070* (2007).

[44] R. Atre, P. K. Panigrahi, and G. S. Agarwal, Phys. Rev. E **73**, 056611 (2006).

[45] Q. Xie, and W. Hai, Phys. Rev. A **75**, 015603 (2007).

[46] Utpal Roy, and P. K. Panigrahi, *cond-mat/0703092* (2007).

[47] U. Al Khawaja, *arXiv: 0706.2705* (2007).

[48] W. Hai, Y. Li, B. Xia, and X. Luo, Eur. Phys. Lett. **71**, 28 (2005).

Chapter 6

Coherent states of Pöschl-Teller potential and their revival dynamics

A recently developed algebraic approach for constructing coherent states for solvable potentials is used to obtain the displacement operator coherent state of the Pöschl-Teller potential. We establish the connection between this and the annihilation operator coherent state and compare their properties. We study the details of the revival structure arising from different time scales underlying the quadratic energy spectrum of this system.

6.1 Introduction

Since its introduction by Schrödinger [1], coherent states (CSs) have attracted considerable attention in the literature [2, 3, 4, 5, 6, 7]. A variety of coherent states, e.g., minimum uncertainty coherent state (MUCS), annihilation operator coherent state (AOCS), displacement operator coherent state (DOCS) and recently Klauder type CS [4], possessing temporal stability, have been constructed and applied to diverse physical phenomena [3]. Coherent states of systems possessing nonlinear energy spectra are of particular interest as their temporal evolution can lead to revival and fractional revival, leading to the formation of Schrödinger cat and cat-like states [8, 9, 10]. A celebrated example in quantum optics of the aforementioned phenomenon is the coherent state in a Kerr type nonlinear medium [11]. In quantum mechanical potential problems, Hamiltonians for potentials

like, Pöschl-Teller, Morse and Rosen-Morse (RM) lead to nonlinear spectra. Time evolution of the CSs for these potentials, a subject of considerable current interest [12, 13, 14, 15, 16, 17, 18, 19, 20, 21, 22], can produce the above type of states.

The simplest way to construct CSs is a symmetry based approach [5]. It is well-known that making use of the Heisenberg algebra $[a, a^\dagger] = 1$, one can construct all the above type of CSs for the Harmonic oscillator, which are identical to each other. In many physical problems, groups like SU(2) and SU(1,1) manifest naturally, enabling a straightforward construction of CSs. For the identification of the symmetry structure of quantum mechanical potential problems, recourse has been taken to a number of approaches, starting from the factorization property of the corresponding differential equations. For the so called shape invariant potentials, super symmetric (SUSY) quantum mechanics [23] based raising and lowering operators have found significant application. A Klauder type CS, using a matrix realization of the ladder operators, has also been constructed [4]. The fact that, SUSY ladder operators act on the Hilbert space of different Hamiltonians, has led to difficulties [15] in proper operator identification of the symmetry generators. The ladder operators have been taken to be functions of quantum numbers, which makes the corresponding algebraic structure ambiguous. This, in turn, creates difficulty in establishing a precise connection between the complete set of states describing the CS and the symmetry of the potential under consideration. In a number of approaches an additional angular variable have been employed [24] to identify SU(1,1) type algebras for describing the infinite number of states of some of these potentials. Taking advantage of the shape invariance property, quantum group type algebras have also been used for describing the Hilbert spaces [25].

Recently, a general procedure for constructing CSs for potential problems have been developed by some of the present authors [26]. The approach makes use of novel exponential forms of the solutions of the differential equations associated with these potentials for identifying the symmetry generators [27]. No additional variables are introduced and unlike SUSY based approaches one stays in the Hilbert space of a given quantum problem while unravelling its symmetry structure. The present chapter makes use of this approach to study the DOCS of the

Pöschl-Teller potential. The primary motivation for considering the Pöschl-Teller potential is two-fold. First of all, it has a quadratic spectrum leading to a rich revival structure for its CS, which can lead to the formation of cat-like states. Secondly, many other potentials can be obtained from the Pöschl-Teller potential by appropriate limiting procedure and point canonical transformations. Hence, the CSs obtained in this case may have relevance to other potentials. The temporal evolution, auto-correlation and quantum carpet structures [8, 10, 28] of the CSs are carefully analyzed for delineating their structure and various time scales present in this problem. These properties are then contrasted with the corresponding ones of the AOCS [26].

The chapter is organized as follows. In the following section, we briefly outline the procedure to identify the symmetry generators for quantum mechanical potential problems, based on hypergeometric and confluent hypergeometric equations. These symmetry generators are then used for constructing the DOCS for general quantum mechanical potential problems. Dual nature of the DOCS with the AOCS is algebraically established. In Section 6.3, the DOCS for the Pöschl-Teller potential is constructed and its properties studied. We identify and analyze the various time scales of the system in Section 6.4 and compare the quantum evolution of the CS with the classical motion.

6.2 Algebraic structure of quantum mechanical potential problems

As is well-known, the Schrödinger equation for a number of solvable potentials can be connected with the hypergeometric (HG) and confluent hypergeometric (CHG) differential equations (DEs). For example, harmonic oscillator, Coulomb and Morse potentials belong to the CHG class, whereas Pöschl-Teller and Rosen-Morse belong to the HG class. Below, we briefly outline the steps of a novel procedure for solving DEs which connects the solution of a DE with the space of monomials [29]. This is subsequently used for identifying the symmetry generators underlying quantum mechanical potential problems.

A single variable linear differential equation can be easily cast in the form,

$$[F(D) + P(x, d/dx)]y(x) = 0 \tag{6.1}$$

where the first part $F(D)$ is a function of the Euler operator $D = xd/dx$, possibly including a constant term and $P(x, d/dx)$ contains all other operators present in the DE under study. The solution can be written in the form,

$$y(x) = C_\lambda \sum_{n=0}^{\infty} (-1)^n \left[\frac{1}{F(D)} P(x, d/dx)\right]^n x^\lambda , \tag{6.2}$$

with the constraint $F(D)\, x^\lambda = 0$ [29]. Using Eq. (7.18) the polynomial solutions of the HG and CHG can be written in closed form exponential forms [27]:

$${}_2F_1(-n, b; c; x) = (-1)^n \frac{\Gamma(b+n)\Gamma(c)}{\Gamma(c+n)\Gamma(b)} e^{\frac{1}{(D+b)} P(x, \frac{d}{dx})} x^n , \tag{6.3}$$

and

$${}_1F_1(-n; c; x) = (-1)^n \frac{\Gamma(c)}{\Gamma(c+n)} e^{P(x, \frac{d}{dx})} x^n . \tag{6.4}$$

The exponential forms of these solutions are ideal for identifying algebraic structures of the solution spaces. For that purpose, one first identifies raising and lowering operators in the space of monomials. The operators at the level of polynomials can be obtained through similarity transformations. The simplest lowering operators at the level of monomial for CHG and HG functions can be taken [27] as

$$K_- = x\frac{d^2}{dx^2} + c\frac{d}{dx}, \quad and \quad \bar{K}_- = \frac{1}{(D+b)}(x\frac{d^2}{dx^2} + c\frac{d}{dx}), \tag{6.5}$$

respectively. The only criterion in choosing these operators at the monomial level is that, these do not lead to divergent expressions after the similarity transformation. It can be easily shown that, for the CHG case, the following generator form a SU(1,1) algebra at the monomial level:

$$K_- = x\frac{d^2}{dx^2} + c\frac{d}{dx}, \quad K_+ = x, \quad and\ K_3 = x\frac{d}{dx} + \frac{c}{2}. \tag{6.6}$$

Similarly, for the HG case, the SU(1,1) generators are given as,

$$\begin{aligned} \bar{K}_- &= \frac{1}{(D+b)}(x\frac{d^2}{dx^2} + c\frac{d}{dx}), \\ \bar{K}_+ &= (D+b-1)x, \ \ and\ \ K_0 = x\frac{d}{dx} + \frac{c}{2}. \end{aligned} \tag{6.7}$$

Modulo a normalization, the DOCS for the HG type DE can be written, at the monomial level, as

$$\Phi^{\beta}(x) = e^{\beta \bar{K}_+} x^0, \tag{6.8}$$

Here, $x^0 = 1$ is the fiducial state satisfying,

$$\bar{K}_- x^0 = 0. \tag{6.9}$$

To find the CS $\chi(x,\beta)$ at the level of the polynomial, we make use of the exponential form of the solution in Eq. (6.3). The DOCS, $\chi(x,\beta)$, can then be written as,

$$\begin{aligned}
\chi(x,\beta) &= e^{-\bar{K}_-} e^{\beta \bar{K}_+} x^0 \\
&= e^{-K_-} \sum_{n=0}^{\infty} \frac{\beta^n}{n!} [(D+b-1)x]^n x^0 \\
&= \sum_{n=0}^{\infty} \frac{\beta^n}{n!} \frac{\Gamma(b+n)}{\Gamma(b)} e^{-K_-} x^n \\
&= \sum_{n=0}^{\infty} \frac{\beta^n}{n!} (-1)^n \frac{\Gamma(c+n)}{\Gamma(c)} \, {}_2F_1(-n,b,c,x) \, .
\end{aligned} \tag{6.10}$$

It is worth noting that, since the similarity transformation does not affect the algebraic structure, the SU(1,1) algebras remain intact at the polynomial level, albeit with different expressions for the generators.

It is interesting to note that, at the monomial level, the DOCS found above is nothing but the AOCS of $\tilde{K}_-$, i.e. $\tilde{K}_- \Phi^{\beta}(x) = \beta \Phi^{\beta}(x)$, where

$$\tilde{K}_- = \frac{1}{(D+b)(D+c)} \left(x \frac{d^2}{dx^2} + c \frac{d}{dx} \right). \tag{6.11}$$

One notices that $\left[\tilde{K}_-, \bar{K}_+\right] = 1$. Hence, the above procedure is akin to the oscillator construction of AOCS. We can also identify a $\tilde{K}_+$, which leads to the oscillator algebra $\left[\bar{K}_-, \tilde{K}_+\right] = 1$:

$$\tilde{K}_+ = \left(\frac{D+b-1}{D+c-1} \right) x. \tag{6.12}$$

The AOCS considered earlier [26], is the eigen state of $\bar{K}_-$ and is of the form $e^{\beta \tilde{K}_+} x^0$. This relationship between DOCS and AOCS has been referred earlier as

duality of these two type of CSs [30]. Thus far, the specific nature of the potential has not been invoked. Now, we shall use this form to find out the CS for Pöschl-Teller (PT) potentials.

6.3 Coherent state for the symmetric-Pöschl-Teller potential

The trigonometric Pöschl-Teller potential belongs to the HG class having an infinite number of bound states. Hence it is natural to expect an underlying SU(1,1) algebra as its spectrum generating algebra. In reference [26] AOCS of the Pöschl-Teller potential has been constructed, making use of a novel exponential form of the solution of the hypergeometric differential equation. Below we will concentrate on the construction of DOCS, following the same procedure and study its properties. We also compare the properties of DOCS and AOCS.

The eigen values and eigen functions [31] of the symmetric-Pöschl-Teller potential

$$V_{SPT}(y) = \frac{\hbar^2\alpha^2}{2m}\left[\frac{\rho(\rho-1)}{\cos^2\alpha y}\right], \quad \rho > 1, \tag{6.13}$$

are given by,

$$\begin{aligned} E_n^{SPT} &= \frac{\hbar^2\alpha^2}{2m}(n+\rho)^2, \quad n = 0,1,2,\ldots \text{ and} \\ \Psi_n^{SPT}(\bar{x}) &= \left[\frac{\alpha(n!)(n+\rho)\Gamma(\rho)\Gamma(2\rho)}{\sqrt{\pi}\Gamma(\rho+\frac{1}{2})\Gamma(n+2\rho)}\right]^{\frac{1}{2}}(1-\bar{x}^2)^{\frac{\rho}{2}}C_n^{\rho}(\bar{x}), \end{aligned} \tag{6.14}$$

with $\bar{x} = \sin\alpha y$. Using the relation [32]

$$C_n^{\rho}(1-2x) = \frac{\Gamma(2\rho+n)}{\Gamma(2\rho)\Gamma(n+1)}\,{}_2F_1(-n,b,c,x) \tag{6.15}$$

and $\bar{x} = 1-2x$, where $b = 2\rho+n$ and $c = \rho+1/2$, we obtain from Eq. (6.10)

$$\chi(\bar{x},\beta) = \sum_{n=0}^{\infty}\frac{(-\beta)^n}{n!}\left[\frac{\Gamma(\rho+n+1/2)\Gamma(2\rho)}{\Gamma(2\rho+n)\Gamma(\rho+1/2)}\right]C_n^{\rho}(\bar{x}) \tag{6.16}$$

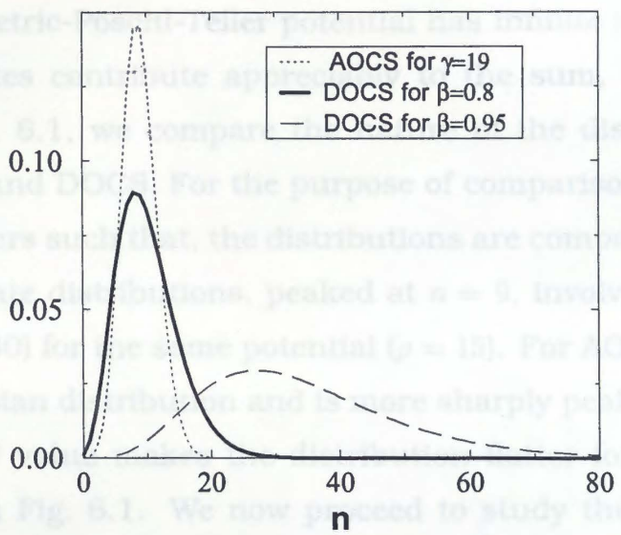

Figure 6.1: The $|d_n|^2$ plots of DOCS and AOCS of symmetric-Pöschl-Teller potential for $\rho = 15$.

Now multiplying Eq. (6.16) by $(1-\bar{x}^2)^\rho/2$ and comparing with Eq. (6.14), we get the coherent state in energy eigenfunction basis as,

$$\bar{\chi}(\bar{x},\beta) = \sum_{n=0}^{\infty} d_n \Psi_n^{\mathrm{SPT}}(\bar{x}) \ , \tag{6.17}$$

where

$$d_n = (-\beta)^n \left[\frac{\Gamma(\rho+n+1/2)^2}{\Gamma(2\rho+n)\Gamma(n+1)(n+\rho)}\right]^{1/2} . \tag{6.18}$$

For comparison, the eigen function distribution for AOCS can be written as

$$d_n^{AOCS} = (\gamma)^n \left[\frac{1}{\Gamma(2\rho+n)\Gamma(n+1)(n+\rho)}\right]^{1/2} . \tag{6.19}$$

We can also obtain the DOCS of a general trigonometric Pöschl-Teller potential [4] modulo a normalization factor, in the same manner as for the symmetric-Pöschl-Teller case :

$$\chi^{PT}(\bar{x},\beta) = \sum_{n=0}^{\infty} d_n^{PT} \, \psi_n^{PT}(\bar{x}) \tag{6.20}$$

where

$$\begin{aligned} d_n^{PT} &= (-\beta)^n \left[\frac{\Gamma(k+n+1/2)\Gamma(\rho+n+1/2)}{(k+\rho+2n)\Gamma(n+1)\Gamma(k+\rho+n)}\right]^{1/2}, \\ \Psi_n^{PT}(\bar{x}) &= \left[\frac{2\alpha(k+\rho+2n)\Gamma(n+1)\Gamma(k+\rho+n)}{\Gamma(k+n+1/2)\Gamma(\rho+n+1/2)}\right]^{1/2} \\ &\times \ (1-\bar{x})^{\rho/2}(\bar{x})^{k/2} P_n^{k-1/2,\rho-1/2}(1-2\bar{x}). \end{aligned} \tag{6.21}$$

Although the symmetric-Pöschl-Teller potential has infinite number of bound states, only a few states contribute appreciably to the sum, which is peaked around $n = \bar{n}$. In Fig. 6.1, we compare the nature of the distributions of the eigen states for AOCS and DOCS. For the purpose of comparison, we have taken the coherence parameters such that, the distributions are comparable. It is found that, both the eigen state distributions, peaked at $n = 9$, involve the same eigen states (from n=0 to n=30) for the same potential ($\rho = 15$). For AOCS, the distribution resembles a Gaussian distribution and is more sharply peaked, as compared to the DOCS. Larger β value makes the distribution flatter for DOCS, as seen in the dashed curve in Fig. 6.1. We now proceed to study the spatio-temporal dynamics of these wave packets.

6.4 Revival dynamics of coherent state

The time evolution of CS $\chi(\bar{x}, \beta)$ can be written as

$$\chi(\bar{x}, t) = \sum_{n=0}^{\infty} d_n \psi_n(\bar{x}) e^{-iE_n t}. \tag{6.22}$$

As the energy expression contains terms up to n^2, the system shows revival and fractional revival but no super-revival phenomenon. All graphs are plotted in time, scaled by the revival time $T_{rev} = 4\pi/\alpha^2$, .

In order to throw more light on the structure of the revival pattern, we note that the eigen functions satisfy

$$\psi_n(-\bar{x}) = (-1)^n \psi_n(\bar{x}). \tag{6.23}$$

From Eq. (6.22), we can easily obtain the CS wave packet at time $t = 1/2\ T_{rev}$ as

$$|\chi(\bar{x}, t = \frac{1}{2} T_{rev})|^2 = |\chi(-\bar{x}, t = 0)|^2. \tag{6.24}$$

Thus, at time $t = 1/2\ T_{rev}$, a mirror image of the initial wave packet is produced at the opposite end of the potential well (Fig. 6.2 and 6.3). This can be observed as a bright ray at time $t = 1/2\ T_{rev}$, in the quantum carpet structure (Fig. 6.4). The auto-correlation function

$$A(t) = \langle \chi(\bar{x}, t) | \chi(\bar{x}, 0) \rangle, \tag{6.25}$$

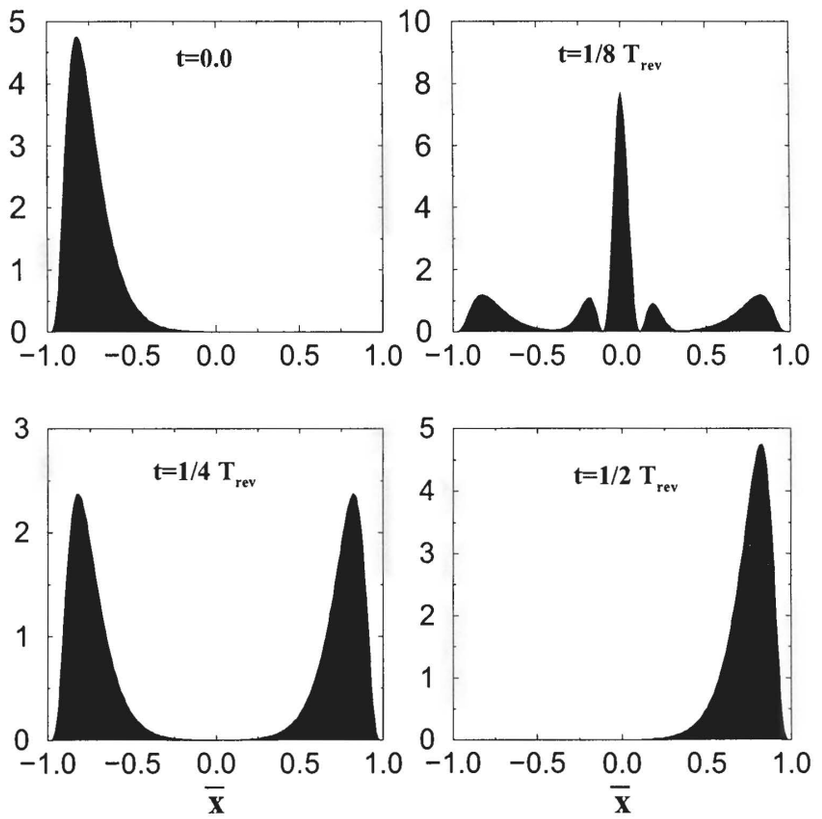

Figure 6.2: Probabity density plot of DOCS of symmetric-Pöschl-Teller potential at different times for $\beta = 0.8$ and $\rho = 10$.

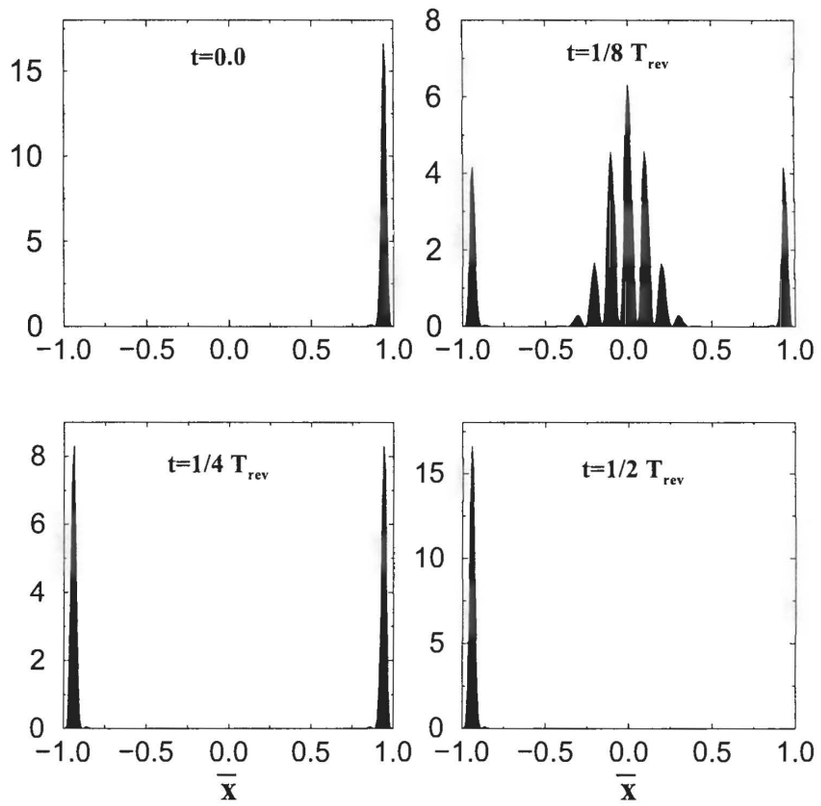

Figure 6.3: Probabity density plot for AOCS of symmetric-Pöschl-Teller potential at different times for $\beta' = 30$ and $\rho = 10$.

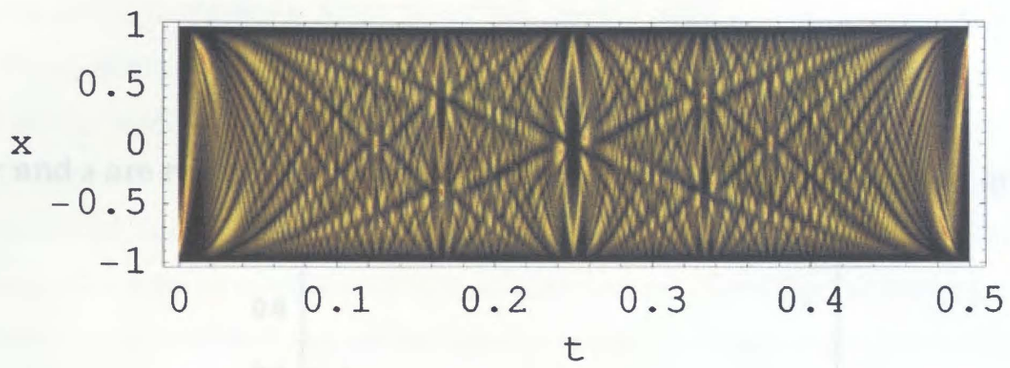

Figure 6.4: Quantum carpet of the displacement operator coherent state of symmetric-Pöschl-Teller potential for $\beta = 0.8$ and $\rho = 10$, brightness signifies the maximum.

yields

$$A(t = 1/2) = \sum_{(A+n)\ even} |d_n|^2 - \sum_{(A+n)\ odd} |d_n|^2 . \tag{6.26}$$

As d_n oscillates rapidly, it will not contribute significantly to the $|A(t)|^2$ (Fig. 6.5), at $t = 1/2\ T_{rev}$. At time $t = 1/4\ T_{rev}$ the CS wave packet becomes

$$\begin{aligned} \chi(\bar{x}, \frac{1}{4}T_{rev}) &= \frac{1}{\sqrt{2}} e^{-i\pi/4} \left[\chi(\bar{x}, 0) + e^{i\pi/2}\chi(-\bar{x}, 0)\right] \\ |\chi(\bar{x}, \frac{1}{4}T_{rev})|^2 &= \frac{1}{2}\left[|\chi(\bar{x}, 0)|^2 + |\chi(-\bar{x}, 0)|^2\right] \end{aligned} \tag{6.27}$$

In this case, the wave packet breaks up into two parts which are situated at the two opposite corners of the potential well (Fig. 6.2 and 6.3). This gives rise to two bright spots at the two vertical ends of the quantum carpet at $t = .25$. At the same instance, the auto-correlation function only gives a peak, as manifested in Fig. 6.5. To explain the probability density plot at $t = 0.125$, we consider a fictitious classical wave packet

$$\chi_{cl}(\bar{x}, t) = \sum_{n=0}^{\infty} d_n\, \psi_n(\bar{x}) e^{-2\pi i \frac{n}{T_{cl}} t} , \tag{6.28}$$

which behaves like the initial wave packet at small time (order of T_{cl}) where $T_{cl} = \frac{2\pi}{\alpha^2\rho}$. Using the discrete Fourier transform (DFT), the original CS wave packet (Eq. (6.22)) at time $t = \frac{r}{s}T_{rev}$ can be written as a linear combination of classical wave packet of Eq. (6.28) as

$$\chi(\bar{x}, \frac{r}{s}T_{rev}) = \sum_{p=0}^{l-1} a_p\, \chi_{cl}(\bar{x}, \frac{r}{s}T_{rev} + \frac{p}{l}T_{cl}) , \tag{6.29}$$

where

$$a_p = \frac{1}{l}\sum_{n=0}^{l-1} \exp\left[2\pi i(n\frac{p}{l} - n^2\frac{r}{s})\right] . \tag{6.30}$$

Here, r and s are two mutually prime integers and l is the period of the quadratic

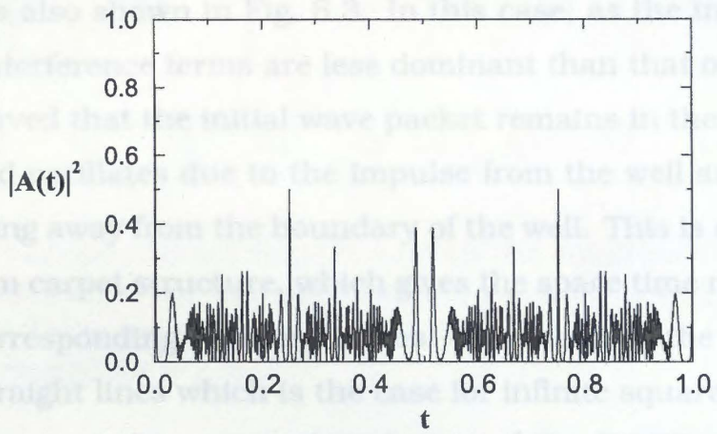

Figure 6.5: Plot of square modulus $|_{SPT}\langle\chi(x,t)|\chi(x,0.)\rangle_{SPT}|^2$ of the auto correlation function of DOCS as a function of time, for $\beta = 0.8$, $\rho = 10$.

phase term. In general, $l = \frac{s}{2}$, if s is integral multiple of 4 and $l = s$ in all other cases. In this case $\frac{r}{s} = \frac{1}{8}$ and $l = \frac{s}{2} = 4$, Substituting in Eq. (6.29) and Eq. (6.30), we get

$$\chi(\bar{x}, \frac{1}{8}T_{rev}) = a_0\,\chi_{cl}^{(0)} + a_1\chi_{cl}^{(1)} + a_2\chi_{cl}^{(2)} + a_3\chi_{cl}^{(3)} \tag{6.31}$$

where

$$\chi_{cl}^{(i)} = \chi_{cl}(\bar{x}, \frac{1}{8}T_{rev} + \frac{i}{4}T_{cl}), \quad i = 0,1,2,3 \tag{6.32}$$

and $a_0 = -a_2 = \frac{1}{2\sqrt{2}}(1-i)$; $a_1 = a_3 = 1/2$.

The above expression (6.31) signifies that the wave packet has broken into four parts, each of them differing by a phase $\pi/4$. In the probability density

$$|\chi(t=\frac{1}{8})|^2 = \frac{1}{4}\left[|\chi_{cl}^1|^2 + |\chi_{cl}^2|^2 + |\chi_{cl}^3|^2 + |\chi_{cl}^4|^2\right] \tag{6.33}$$

$$+\frac{1}{2}\mathrm{Re}\left[\chi_{cl}^{1\,*}\chi_{cl}^2 e^{i\pi/4} - \chi_{cl}^{1\,*}\chi_{cl}^3 + \chi_{cl}^{1\,*}\chi_{cl}^4 e^{i\pi/4} - \chi_{cl}^{2\,*}\chi_{cl}^3 e^{-i\pi/4} + \chi_{cl}^{2\,*}\chi_{cl}^4 - \chi_{cl}^{3\,*}\chi_{cl}^4 e^{i\pi/4}\right], \tag{6.34}$$

the first term carries the contribution from the individual subsidiary waves and the second term arises due to the interference between them. We note that the χ_{cl}^1 and χ_{cl}^3 are spatially well separated, giving very less contribution in interference.

The dominant interference term is $\chi_{cl}^{2^*}\chi_{cl}^{4}$, as χ_{cl}^{2} and χ_{cl}^{4} are not spatially separated. Thus, at time $t = 0.125$, wave function splits into four parts, but their interference at the middle gives a strong peak, rather than giving four distinct similar waves. For comparison, the wave packet structure for AOCS of symmetric-Pöschl-Teller potential is also shown in Fig. 6.3. In this case, as the initial wave packet is sharper, the interference terms are less dominant than that of DOCS.

We have observed that the initial wave packet remains in the left corner of the potential well and oscillates due to the impulse from the well and at later times, as it spreads, being away from the boundary of the well. This is quite transparent from the quantum carpet structure, which gives the space time rays of probability density of the corresponding coherent states. We note that, the rays in quantum carpet are not straight lines which is the case for infinite square-well.

In order to contrast the temporal evolution of the DOCS with the classical motion, we note that for a particle of energy E,

$$x(t) = a \arccos\left[\frac{\alpha_1 - \beta_1}{2} + \sqrt{\Delta}\cos\left(\sqrt{\frac{2E_c}{m}}\frac{t}{a}\right)\right] \tag{6.35}$$

where $\Delta = (1-\frac{1}{2}(\sqrt{\alpha_1}+\sqrt{\beta_1})^2)(1-\frac{1}{2}(\sqrt{\alpha_1}-\sqrt{\beta_1})^2)$, $V_0 = \frac{\alpha^2}{m}$ and $\alpha_1 = \frac{V_0}{E_c}\rho(\rho-1)$, $\beta_1 = \frac{V_0}{E_c}k(k-1)$; with the condition

$$E_c > \frac{V_0}{2}(\sqrt{\rho(\rho-1)} + \sqrt{k(k-1)})^2. \tag{6.36}$$

This classical trajectory is shown in Fig. 6.6(b). The expectation value of the position with respect to the coherent state of general trigonometric Pöschl-Teller potential is obtained as

$$\langle x(t)\rangle = \frac{1}{\alpha}\arcsin\sqrt{1/2\,(1-z)} \tag{6.37}$$

where

$$z = N\sum_{n=0}^{\infty}(2A_n\,\cos\left[2\,\alpha^2(2n+\rho+k+1)t\right] - C_n)$$

having,

$$A_n = -(\beta)^{2n+1}\left[\frac{2\Gamma(\rho+n+3/2)\Gamma(k+n+3/2)}{\Gamma(\rho+k+n)\Gamma(n+1)(2n+\rho+k)(2n+\rho+k+1)(2n+\rho+k+2)}\right]$$

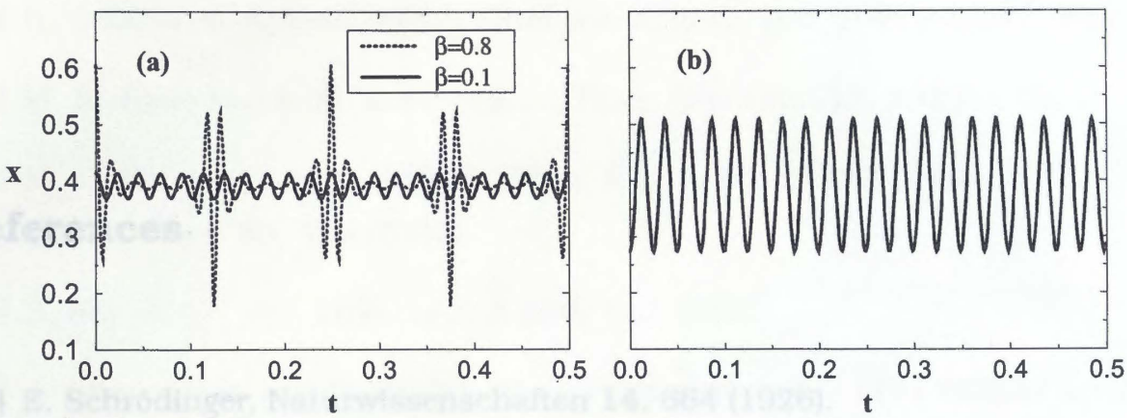

Figure 6.6: Plots of expectation values of x for (a) the coherent state of the Pöschl-Teller potential, with different values of β where $\rho = 5, k = 5$ and $\alpha = 2$.(b) classical solution of Pöschl-Teller potential, with $a = 0.25, m = 1, V_0 = 4, k = 5, \rho = 5$ and $E_c =$ average value of energy for $\beta = 0.1$.

and

$$C_n = (\beta)^{2n}\left[\frac{\Gamma(\rho+n+1/2)\Gamma(k+n+1/2)(k+\rho-1)(k-\rho)}{\Gamma(\rho+k+n)\Gamma(n+1)(2n+\rho+k)(2n+\rho+k-1)(2n+\rho+k+1)}\right]$$

N being the normalization constant. This $\langle x(t)\rangle$ is plotted in Fig. 6.6(a) which nearly matches with the classical trajectory for very small values of β (solid line in Fig. 6.6(a)). In this case only a few eigen states contribute to the coherent state wave packet. Sudden changes in the $\langle x(t)\rangle$ values are the signatures of revivals and the fractional revivals [33].

References

[1] E. Schrödinger, Naturwissenschaften **14**, 664 (1926).

[2] R. J. Glauber, Phys. Rev. **130**, 2529 (1963); R. J. Glauber, Phys. Rev. Lett. **10**, 84 (1963); R. J. Glauber, Phys. Rev. **131**, 2766 (1963); J. R. Klauder J. Math. Phys. **4**, 1055 (1963); J. R. Klauder, Phys. Rev. Lett. **16**, 534 (1966).

[3] J. R. Klauder and B. S. Skagerstam, *Coherent States: Applications in Physics and Mathematical Physics* (World Scientific, Singapore, 1985).

[4] J. R. Klauder, J. Phys. A: Math. Gen. **29**, L293 (1996); J. P. Gazeau and J. R. Klauder, J. Phys. A: Math. Gen. **32**, 123 (1999); J. P. Antoine *et al.*, J. Math. Phys. **42**, 2349 (2001) and references therein.

[5] A. M. Perelomov, *Generalized Coherent States and Their Applications* (Springer, Berlin, 1986).

[6] W. M. Zhang, D. H. Feng and R. Gilmore, Rev. Mod. Phys. **62**, 867 (1990) and references therein.

[7] G. S. Agarwal, *Selected Papers on Fundamentals of Quantum Optics* (SPIE milestone series) 103.

[8] I. Sh Averbukh and N. F. Perelman, Phys. Lett. A **139**, 449 (1989); J. Banerji and G. S. Agarwal, Phys. Rev. A **59**, 4777 (1999); M. J. W. Hall, M. S. Raineker and W. P. Schleich, J. Phys. A: Math. Gen. **32**, 8275 (1999); A. E. Kaplan *et al.*, Phys. Rev. A **61**, 032101 (2000).

[9] R. Bluhm, V. A. Kostelecky, and J. Porter, Am. J. Phys. **64**, 944 (1996).

[10] M. A. Doncheski and R. W. Robinett, Phys. Rep. **392**, 1 (2004) and references therein

[11] K. Tara, G. S. Agarwal and S. Chaturvedi, Phys. Rev. A **47**, 5024 (1993).

[12] M. M. Nieto and L. M. Simmons Jr., Phys. Rev. Lett. **41**, 207 (1978).

[13] M. G. Benedict and B. Molnár, Phys. Rev. A **60**, R1737 (1999); S. H. Dong, Can. J. Phys. **80**, 129 (2002).

[14] B. Roy and P. Roy, Phys. Lett. A **296**, 187 (2002).

[15] A. Chenaghlou and H. Fakhri, Mod. Phys. Lett. A **17**, 1701 (2002); A. Jellal, Mod. Phys. Lett. A **17**, 671 (2002); H. Fakhri and A. Chenaghlou, Phys. Lett. A **310**, 1 (2003).

[16] E. A. Shapiro, M. Spanner and M. Y. Ivanov, Phys. Rev. Lett. **91**, 237901 (2003).

[17] M. M. Nieto, Phys. Rev. A **17**, 1273 (1978).

[18] M. M. Nieto and L. M. Simmons, Jr., Phys. Rev. D **20**, 1332 (1979); M. M. Nieto and L. M. Simmons, Jr., Phys. Rev. D **20**, 1342 (1979).

[19] M. G. A. Crawford and E. R. Vrscay, Phys. Rev. A **57**, 106 (1998).

[20] A. H. Kinani and M. Daoud, Phys. Lett. A **283**, 291 (2001).

[21] M. M. Nieto, Mod. Phys. Lett. A **16**, 2305 (2001).

[22] Y. Hassouni, E. M. F. Curado and Rego-Monteiro, Phys. Rev. A **71**, 022104 (2005).

[23] F. Cooper, A. Khare and U. P. Sukhatme, Phys. Rep. **251**, 268 (1995); F. Cooper, A. Khare and U. P. Sukhatme *Supersummetry in Quantum Mechanics* (World Scientific, Singapore, 2001).

[24] A. Gangopadhyaya, J. V. Mallow and U. P. Sukhatme, Phys. Rev. A **58**, 4287 (1998); J. Wu and Y. Alhassid, J. Math. Phys. **31**, 557 (1990); J. Wu, Y. Alhassid and F. Gürsey, Ann. Phys. **196**, 163 (1989).

[25] A. N. F. Aleixo and A. B. Balantekin, *quant-ph*/0407160 (2004) and references therein.

[26] T. Shreecharan, P. K. Panigrahi and J. Banerji, Phys. Rev. A **69**, 012102 (2004).

[27] N. Gurappa N, P. K. Panigrahi and T. Shreecharan, J. Comput. Appl. Math. **160**, 103 (2003).

[28] W. Loinaz and T. J. Newman, J. Phys. A: Math. Gen. **32**, 8889 (1999).

[29] N. Gurappa and P. K. Panigrahi, *ibid.* **67**, 155323 (2003).

[30] P. Shanta *et al.*, Phys. Rev. Lett. **72**, 1447 (1994).

[31] C. Quesne, J. Phys. A: Math. Gen. **32**, 6705 (1999).

[32] I. S. Gradshteyn and I. M. Ryzhik, *Table of Integrals, Series and Products* (Academic Press, USA, 2000); M. Abramowitz and I. A. Stegan, *Handbook of Mathematical Functions* (Dover, New York, 1970).

[33] C. Sudheesh, S. Lakshmibala and V. Balakrishnan, Phys. Lett. A **329**, 14 (2004).

Chapter 7

Sinusoidal excitations in reduced Maxwell-Duffing model

Sinusoidal wave solutions are obtained for reduced Maxwell-Duffing equations describing the wave propagation in a non-resonant atomic medium. These continuous wave excitations exist when the medium is initially polarized by an electric field. Other obtained solutions include both mono-frequency and cnoidal waves.

7.1 Introduction

An atomic medium in general conditions is modelled by N-level atoms. In the two-level resonant approximation, the system is characterized by the Bloch equations, which is inaccurate in several physical situations [1, 2], like dense atomic media and systems involving three or more level atoms. Thus the resonant model needs to be generalized and extended to the non-resonant scenario. One of the well studied approaches is to consider the response of the medium as weakly nonlinear. Such situation leads to the Duffing oscillator model, where the nonlinear response of the medium is assumed to be cubic. This is the simplest generalization of the Lorentz model.

On the other hand, Maxwell wave equation, for a linearly polarized light, allows propagation in both the directions. However, this can be approximated to unidirectional wave propagation when anharmonic contribution to the polarization is very small. As a result, the wave equation reduces from second order to a first order equation. For a non-resonant medium, this approximation results in the reduced Maxwell-Duffing model (RMD).

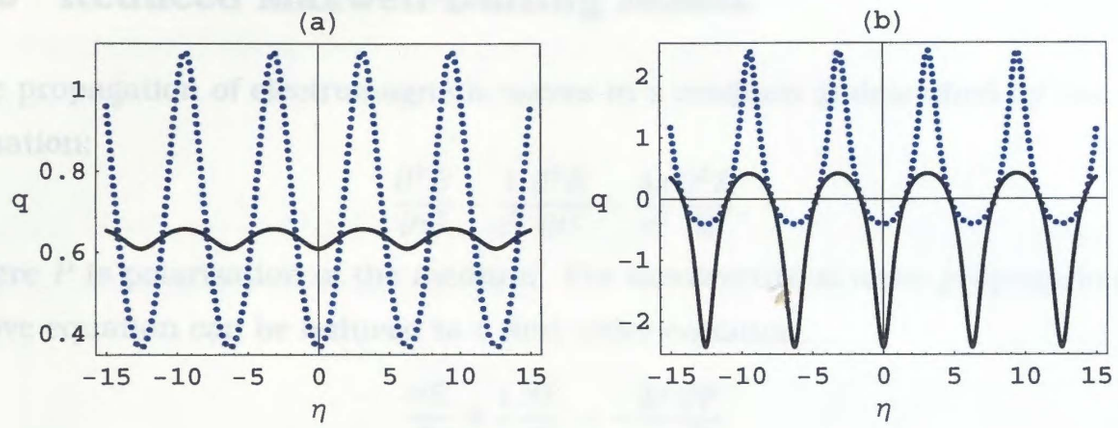

Figure 7.1: Mono-frequency solutions for $\mu = 0.5$ with (a) $\alpha = 1.6$ and (b) $\alpha = 3.0$. The second case implies $A = 0$.

Different excitations in non-resonant atomic media are currently attracting considerable attention, because of their relevance to ultra-short regime. Detailed reviews of various aspects of non-linear excitations in atomic media can be found in [3, 4]. In case of two level atoms, the localized soliton solutions of the Maxwell-Bloch equations explained the physical phenomenon of self-induced transparency [5]. In the same system, general cnoidal waves have also been found as exact solution [6, 7, 8]. It was observed [9] that, these waves can be naturally excited in the presence of relaxation. Such shape preserving Jacobi elliptic pulse train solutions have been experimentally observed [10]. More general periodic solutions in multi-level systems have also been reported [11].

In case of Maxwell-Duffing model, a class of exact localized soliton solutions have been recently obtained [12]. We present here mono frequency, sinusoidal wave excitations for RMD system. This excitation exists only in the presence of a polarizing background. General cnoidal wave solutions are found both with and without background.

Below a brief summery of the reduced Maxwell-Duffing model is presented after which a procedure to find exact solutions of this system through a fractional linear transform is outlined. We then present the novel sinusoidal wave solutions including single frequency and cnoidal waves.

7.2 Reduced Maxwell-Duffing Model:

The propagation of electromagnetic waves in a medium is described by the wave equation:

$$\frac{\partial^2 E}{\partial z^2} - \frac{1}{c^2}\frac{\partial^2 E}{\partial t^2} = \frac{4\pi}{c^2}\frac{\partial^2 P}{\partial t^2}. \tag{7.1}$$

where P is polarization of the medium. For unidirectional wave propagation, the above equation can be reduced to a first order equation,

$$\frac{\partial E}{\partial z} + \frac{1}{c}\frac{\partial E}{\partial t} = -\frac{2\pi}{c}\frac{\partial P}{\partial t}. \tag{7.2}$$

In the Duffing oscillators model, the nonlinear response of the medium is cubic. The corresponding equation for the motion of electrons in the presence of an external electric field is given by

$$\frac{\partial^2 X}{\partial t^2} + \omega_0^2 X + \kappa_3 X^3 = \frac{e}{m}E. \tag{7.3}$$

Here X represents the displacement of an electron from its equilibrium position, ω_0 is the oscillator frequency, κ_3 is anharmonicity constant, and m is the effective mass of the electron of charge e. The medium polarization is defined as $P = neX$, where n is the number density of the oscillators in the medium.

We choose new variables $\tau = z/l$, $x = \omega_0(t - z/c)$ and normalize the independent variables as

$$\tilde{e} = E/A_0, q = X/X_0. \tag{7.4}$$

In terms of the new variables, Eq. (7.3) then takes the form

$$\frac{\partial^2 q}{\partial x^2} + q + 2\mu q^3 = \tilde{e}, \tag{7.5}$$

where $2\mu = \kappa_3 X_0^2/\phi_0^2$ and $A_0 = m\omega_0^2 X_0/e = m\omega_0^3 e^{-1}(2\mu/|\kappa_3|)^{1/2}$. X_0 can be expressed as $X_0 = (2\mu\omega_0^2/|\kappa_3|)^{1/2}$. Similarly Eq. (7.2) is transformed to

$$\frac{\partial \tilde{e}}{\partial \tau} = -\frac{\partial q}{\partial x}. \tag{7.6}$$

Here l is defined as

$$l^{-1} = 2\pi n e^2/(mc\phi_0) = \phi_p^2/2c\phi_0, \tag{7.7}$$

where $\omega_p = (4\pi ne^2/m)^{1/2}$ is the plasma frequency. Eq. (7.5) and (7.6) together are called reduced Maxwell-Duffing equations. For finding propagating solutions, one defines

$$\eta = x - \tau/\alpha, \tag{7.8}$$

where α is related to the velocity of the pulse. Eq. (7.6) can be integrated with respect to the single variable η to yield

$$\tilde{e}(t,x) = \alpha q(t,x) + C, \tag{7.9}$$

where C is a constant, which signifies the background electric field, when electron amplitude q goes to zero. Non-linear equation of motion in Eq. (7.5) then takes the form:

$$\frac{d^2q}{d\eta^2} + (1-\alpha)q + 2\mu q^3 = C. \tag{7.10}$$

For a wave propagating in the right direction, $\alpha > 1$ and $\mu > 0$, which is considered below. The other propagation direction can be like wise studied.

7.3 Fractional Linear Transform and the solutions:

The above Eq. (7.10) is in the form, which can be obtained from the real part of the non-linear Schrodinger equation with a source. For finding out explicit solutions we consider Eq. (7.10):

$$q'' + gq^3 + \epsilon q = C, \tag{7.11}$$

provided $g = 2\mu$ and $\epsilon = (1-\alpha)$. Prime indicates differentiation with respect to η. It is known earlier [13], that this equation can be connected to the elliptic equation $f'' + af + bf^3 = 0$ through the following fractional linear transformation (FT):

$$q(\eta) = \frac{A + Bf(\eta,m)^\delta}{1 + Df(\eta,m)^\delta} \tag{7.12}$$

where A, B and D are real constants, δ is an integer, and $f(\eta,m)$ is a Jacobi elliptic function, with the modulus parameter m ($0 \leq m \leq 1$). It can be shown, that $=2$ is the maximum allowed value. Here we concentrate on the periodic solution of Eq. (7.11) for $\delta = 1$ and $q(\eta,m) = cn(\eta,m)$. Solutions for other elliptic functions also can be studied in a similar way.

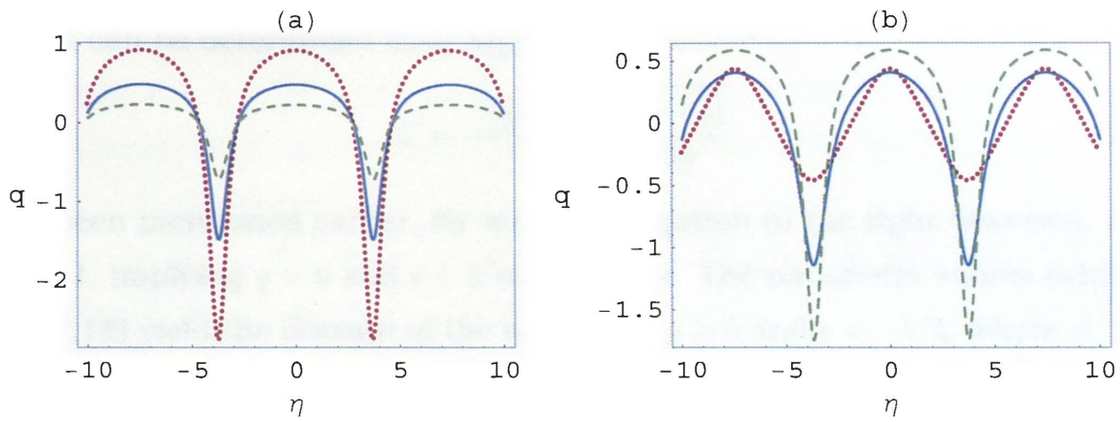

Figure 7.2: Cnoidal wave solution in presence of source. (a) (Dotted line) $g = 2.0$, (solid line) $g = 7.0$ and (dashed line) $g = 30$ for $\epsilon = -5.0$; b) (Dotted line) $\epsilon = -0.001$, (solid line) $\epsilon = -2.0$ and (dashed line) $\epsilon = -5.0$ for $g = 5$.

I. General solution:

i) The consistency conditions for $m = 0$ are given by

$$A^3g + 2D(AD - B) + A\epsilon - C = 0, \tag{7.13}$$

$$3A^2Bg + AD(1 + 2\epsilon) + B(\epsilon - 1) - 3CD = 0, \tag{7.14}$$

$$3AB^2g + AD^2(\epsilon - 1) + BD(1 + 2\epsilon) - 3CD^2 = 0, \tag{7.15}$$

$$B^3g + BD^2\epsilon - CD^3 = 0. \tag{7.16}$$

It should be pointed out that $cn(\eta, 0) = cos(\eta)$. One can see from the above FT (Eq. (7.12)) that $AD = B$ implies only a constant or trivial solution and is not considered here. An $(AD - B)$ factor can be taken out of all the conditions by tactically using the first consistency in Eq. (7.13). Other conditions were used to solve for the unknowns A, B and D. The source term (C) can be determined from the first condition itself. Thus, the solution is expressed as

$$q(\eta) = \frac{A + Bcos(\eta)}{1 + Dcos(\eta)}, \tag{7.17}$$

where, A, B and D respectively are

$$A = \pm\frac{(\epsilon + 2)}{\sqrt{3g(1 - \epsilon)}},\ B = -\sqrt{\frac{-(1 + 2\epsilon)}{6g}},$$

$$and \qquad D = \pm\sqrt{\frac{-(1 + 2\epsilon)}{2(1 - \epsilon)}}. \tag{7.18}$$

After solving the solution parameters, the source term or the constant electric field part can be determined from Eq. (7.13):

$$C = -\frac{(1+2\epsilon)}{3}\sqrt{\frac{(1-\epsilon)}{3g}} \tag{7.19}$$

As has been mentioned earlier, for wave propagation in the right direction, $\mu > 0$ and $\alpha > 1$, implying $g > 0$ and $\epsilon < 0$ respectively. The parameter values exhibited in Eq. (7.18) yield the domain of the solutions: $g > 0$ and $\epsilon < -1/2$, where A, B, D are real and C is a positive quantity. It is worth pointing out that all the solutions are non-singular in nature. This is because the magnitude of D is less than unity. The solutions are depicted in Fig. 7.1 (a) for $\mu = 0.5$ with $\alpha = 1.6$. The dotted line corresponds to the solution for positive value of D and the solid line is for the negative one. The first plot is with a background, *i.e.*, $A \neq 0$.

ii) The consistency conditions, (7.13-7.16) support solution for $A = 0$ if the source is non-zero. In this case, $\epsilon = -2$ and the solution is written as

$$q(\eta) = \pm\frac{1}{\sqrt{g}}\left(\frac{cos(\eta)}{\sqrt{2} \pm cos(\eta)}\right), \tag{7.20}$$

which is plotted in Fig. 7.1 (b) for $\mu = 0.5$ with $\alpha = 3.0$.

iii) Although a wide class of localized pulse propagation is analyzed in [12] for different initial boundary conditions, for completeness we indicate the same for $m = 1$ in the fractional transform. This is expressed as

$$q(\eta) = \frac{A + Bsech(\eta)}{1 + Dsech(\eta)}, \tag{7.21}$$

where

$$A = \pm\sqrt{-\tfrac{(1+\epsilon)}{3g}}$$

$$D = \pm\sqrt{-\tfrac{2(1+\epsilon)}{(1-2\epsilon)}}, \quad and \quad B = \pm\sqrt{\tfrac{2(\epsilon-2)^2}{3g(1-2\epsilon)}} \quad ,$$

with $C^2 = -(1+\epsilon)(1-2\epsilon)^2/(27g)$. This solution exists for $g > 0$ and $\epsilon < -1$. For $\epsilon = 2$, the solution goes to the one, with $B = 0$. All the solutions are non-singular except for $B = 0$ and $D = -\sqrt{2}$, which implies a singular one, signifying self focussing effect.

iv) We now analyze the nature of the solutions in the absence of a polarizing background: $C = 0$. The resultant dynamical equation is the real part of the well

known non-linear Schrödinger equation. In this case, the periodic solution for the electron amplitude is of quadratic fractional type ($\delta = 2$): $A = \sqrt{-8/g}$, $B = 0$, $D = -2$ and $\epsilon = 4$. The solution is singular one, implying an instability in the electron amplitude or the self focussing of the electric field. This happens for any value of $\mu < 0$ and for $\alpha = -3$.

v) In addition to the above mentioned mono-frequency solutions, there are other conoidal wave solutions. As an example, when $m = 1/2$ the consistency conditions are

$$A^3 g + D(AD - B) + A\epsilon - C = 0,$$
$$3A^2 Bg + (2AD + B)\epsilon - 3CD = 0,$$
$$3AB^2 g + D(AD + 2B)\epsilon - 3CD^2 = 0,$$
$$B^3 g + BD^2\epsilon + (AD - B) - CD^3 = 0.$$

These equations lead to,

$$A = \sqrt{\frac{-E}{6g\epsilon}}, \quad B = -\frac{\epsilon}{g}\sqrt{\frac{gF}{3E}}, \quad D = \sqrt{\frac{-F}{2\epsilon}}$$
$$and \quad C = \frac{1}{3\sqrt{6}}\sqrt{-\frac{\epsilon}{g}}\left(\frac{4\epsilon^2 - F}{\sqrt{E}}\right),$$

where $E = 9 + 2\epsilon^2 - 3\sqrt{9 + 4\epsilon^2}$ and $F = \sqrt{9 + 4\epsilon^2} - 3$. E and F are positive for all $\epsilon \neq 0$. These conoidal waves exist in the domain $\epsilon < 0$ and $g > 0$. Solutions are picturised in Fig. 7.2, where the variations of the electron amplitude with g and ϵ are displayed. As μ increases the amplitudes diminish for a fixed value of $\alpha = 6$ (Fig. 7.2(a)). Fig. 7.2(b) shows the nature of the solutions with α for certain value of $\mu = 2.5$.

References

[1] J. Cheng and J. Zhou, Phys. Rev. A **67**, 041404(R) (2003).

[2] C. R. Stroud, Jr., C. M. Bowden and L. Allen, Opt. Commun. **67**, 387 (1988); C. M. Bowden, A. Postan and R. Inguva, J. Opt. Soc. Am. B **8**, 1081 (1991); C. M. Bowden and J. P. Dowling, Phys. Rev. A **47**, 1247 (1993).

[3] R. K. Bullough, P. M. Jack, P. W. Kitchenside and R. Saunders Phys. Scr. **20**, 364 (1979) and references therein.

[4] Th. Brabec and F. Krausz, Rev. Mod. Phys. **72**, 545-591 (2000) and references therein.

[5] S. L. McCall and E. L. Hahn, Phys. Rev. 183, 457 (1969).

[6] J. H. Eberly, Phys. Rev. Lett. **22**, 760 (1969).

[7] L. Matulic, P. W. Milonni and J. H. Eberly, Opt. Commun. **4**, 181 (1971).

[8] L. Allen and J. H. Eberly, *Optical Resonances and Two-Level Atoms* (Dover, New York, 1987) and references therein.

[9] M. A. Newbold and G. J. Salamo, Phys. Rev. Lett. **42**, 887 (1979).

[10] J. L. Shultz and G. J. Salamo, Phys. Rev. Lett. **78**, 855 (1997).

[11] P. K. Panigrahi and G. S. Agarwal, Phys. Rev. A **67**, 033817 (2003).

[12] E. V. Kazantseva, A. I. Maimistov and J. G. Caputo, Phys. Rev. E **71**, 056622 (2005).

[13] T. S. Raju, C. N. Kumar and P. K. Panigrahi *J. Phys. A: Math. Gen.* **38**, L271 (2005).

[14] Y. Chung and T. Schäfer, Phys. Lett. A **361**, 63 (2007).

[15] X. Song, S. Gong, R. Li and Z. Xu, Phys. Rev. A **74**, 015802 (2006).

[16] H. Leblond, S. V. Sazonov, I. V. Mel'nikov, D. Mihalache and F. Sanchez, Phys. Rev. A **74**, 063815 (2006).

Conclusions and Future Outlook

In conclusion, the present thesis deals with the study and development of analytical tools for finding exact solutions of various non-linear systems. For example, we have studied single component cigar shaped Bose-Einstein condensate (BEC) in various scenarios, two-component BEC, non-resonant atomic media and a quantum mechanical system with Pöschl-Teller potential. Coherent control of the nonlinear excitations are also studied in some of the cases. Below, we separately outline the conclusions and future outlook of each work.

In Chap. 2, we have presented a host of exact solutions for the Thomas-Fermi regime of the quasi-one dimensional GP equation. These contain dark soliton, soliton trains, non-singular and singular solutions. A localized solution with a double well density profile has been identified and found to be dynamically stable. We have shown how the depth and the minima locations of the profile can be precisely controlled. This may have utility for trapping of neutral atoms. The effects of time dependent coupling, trap potential and loss on the soliton profile have been addressed exactly. Our procedure can be used to find the effect of many other time dependencies of the parameters on the condensate profile. The propagation of the solitons in time, with above control parameters, have been explicated for a number of physically relevant cases. Solutions in the strong coupling regime is found to be intimately connected with the Lieb-mode of weakly coupled BEC. Study of other nonlinear excitations including Faraday waves and their coherent control, for a radially extended cigar shaped BEC, is currently under investigation. Strongly coupled BEC in an optical lattice is also an interesting area to be studied.

In Chap. 3, complex soliton solutions with power law decay have been identified in the quasi-one-dimensional GP equation with repulsive two- and attractive three-body interactions. These solutions, for which superfluid velocity depends on density, show a slower asymptotic decay compared to the elliptic function type solutions. We have considered the parameters relevant to ^{87}Rb, with the three-body coupling constant in the theoretically predicted range. This opens the possibility of observing these complex solitons in realistic BEC. Soliton velocity is fixed by the strength of the interactions and are stable against small perturbations. They are also modulationally stable. We studied their behaviour in a trap with a loss term. It was found that the nature and character of the solution is not affected by loss. The trap parameters can be used for coherent control of these localized modes.

In Chap. 4, Faraday pattern in Bose Einstein condensates in various interaction regimes are studied, where the Bogoliubov modes are excited through the temporal oscillation of the transverse trap frequency. The solution space of Mathieu equation involving the amplitude of the perturbation is analyzed using the Floquet theorem. This reveals that, series of resonances exist in the system. The dominant wave numbers of the second sound clearly differentiate strong, weak and three-body interactions. These excitations reveal the structure of nonlinearity in the Gross-Pitaevskii equation, governing the mean field dynamics of BEC. For large modulation parameter, this excitations show the bifurcation nature of the system.

In Chap. 5, the two BEC is found to sustain sinusoidal excitations, not possible in the single component case. It is found that appropriate changes in the trap and scattering length can be used to control the profile; the superfluid velocity can also be changed by controlling the experimental parameters. In presence of an optical lattice rich phase structure is observed here. It is found that, there can be dynamical phase transition from superfluid to insulator phases. This can happen for each component separately or in a correlated manner. We note that difference between the ground state energy of the two components can arise be-

cause of the XPM. In the case when the inter-atomic and intra-atomic interactions are of identical strengths, the sinusoidal solutions exist for the same amplitude of the potential. The roles of both harmonic and optical trap together is an area worthy of future investigation. It may provide additional parameters for controlling the dynamical phase transition. One can also study the Faraday patterns in this system with time dependent scattering length. Because of two components, the nature of these excitations will be quite interesting.

In Chap. 6, the algebraic procedure used here, for constructing CSs for potentials based on confluent hypergeometric and hypergeometric differential equations depends on the fact that, the solutions of the above differential equations can be precisely connected with the space of monomials. This leads to a straightforward identification of symmetry generators, without taking recourse to additional angular variables or SUSY type multiple, related Hamiltonians. The nature of the specific potential enters through the corresponding ground states and by fixing the parameters and variables of the above solutions. We have concentrated here on the CS of Pöschl-Teller potential, since various potentials can be obtained from the same, through limiting of parameters and point canonical transformation. The time evolution of the CS for this potential, having non-linear spectra, produces cat like states in fractional revivals. We contrasted the properties of the two different types of CSs possible here, as well as the temporal evolution of the CS, with classical motion. As has been noted earlier, this procedure easily extends to more complicated non-linear coherent states arising from deformed algebras, a subject we intend to take up in future. We also would like to analyze the subject of mesoscopic superposition and sub-Planck scale structure, possible in this type of quantum systems.

In Chap. 7, novel periodic solutions have been obtained for the reduced Maxwell-Duffing model, which are unidirectional, sinusoidal and of mono-frequency character. These solutions complement the localized soliton solutions known in the literature and occur only when a back ground electric field is present. General cnoidal wave solutions are found both with and without back

ground fields. It will be interesting to study the nature of the waves when Maxwell equation is modified by a non-local dispersion term. Polarization properties of the propagating modes should also be investigated in this non-linear medium, as also the nature of the waves when slowly varying amplitude approximation is not valid.

List of Publications

I. Papers in Journals:

1. "Coherent states of the Pöschl-Teller potential and their revival dynamics", Utpal Roy, J. Banerji and P. K. Panigrahi, *J. Phys. A: Math. Gen.* **38**, 9115 (2005).

2. "Coherent control of solitons in strongly coupled cigar shaped BEC", Utpal Roy and P. K. Panigrahi, submitted for publication in Phys. Rev. A.; *arXiv:cond-mat/0703092.*

3. "Complex solitons with power law behaviour in Bose-Einstein condensates near Feshbach resonance", Utpal Roy, R. Atre, C. Sudheesh, C. N. Kumar and P. K. Panigrahi, submitted for publication in Phys. Rev. Lett.; *arXiv:0708.3646.*

4. "Sinusoidal excitations in reduced Maxwell-Duffing model", Utpal Roy, T. S. Raju and P. K. Panigrahi, submitted for publication in Phys. Rev. A.; *arXiv:0711.0449.*

5. "Sinusoidal Excitations in Two Component Bose-Einstein Condensates", P. Das, T. S. Raju, Utpal Roy, and P. K. Panigrahi, submitted for publication in Phys. Rev. A.

6. "Vibrations as probe of Bose-Einstein condensates in different phases", Utpal Roy and P. K. Panigrahi, in preparation.

7. "Bose-Einstein condensates in a harmonic trap with a delta function kick", Utpal Roy and P. K. Panigrahi, in preparation.

II. Papers In Conference Proceedings:

1. On singular solutions of strongly coupled Bose-Einstein condensate, Utpal Roy and P. K. Panigrahi, Proceeding of 2nd International Conference on "Current Developments in Atomic, Molecular and Optical Physics With Applications", held in Delhi University, Delhi, India, March 21-23, 2006.

2. Bose-Einstein condensate with a time varying expulsive trap, Utpal Roy and P. K. Panigrahi, Proceedings of "International Symposium on Quantum Optics", held in Physical Research laboratory, Ahmedabad, India, July 24-27, 2006.

III. Abstract Presented in Conferences/symposiums:

1. SERC School on Quantum Information and Quantum Optics, Physical Research Laboratory, Ahmedabad, India, Feb. 1-14, 2004.

2. XV National Conference on Atomic and Molecular Physics, held in Physical Research Laboratory, Ahmedabad, India, December 20-23, 2004.

3. Workshop on Quantum Information, Computation and Communication (QICC 2005), February 15-18, 2005, Center for theoretical Studies, IIT Kharagpur, India.

4. Topical Conference on Atomic, Molecular and Optical Physics, held in Indian Association for the Cultivation of Science, Kolkata, India, December 13-15, 2005.

5. Current Developments in Atomic, Molecular and Optical Physics With Applications, held in Delhi University, Delhi, India, March 21-23, 2006.

6. International Symposium on Quantum Optics, held in PRL, Ahmedabad, India, July 24-27, 2006.

7. International Conference on Laser and Nanomaterials, held in University of Calcutta, Kolkata, India, November 30-December 2, 2006.

8. XVI National Conference on Atomic and Molecular Physics, Tata Institute of Fundamental Research, Mumbai, India, Jan. 8-11, 2007.

9. The 38th annual meeting of the Division of Atomic, Molecular, and Optical Physics (DAMOP) of the American Physical Society, Calgary, Canada, June 5 - 9, 2007.